NUREG/CR-5208
MEA-2305

Warm Prestress Modeling: Comparison of Models and Experimental Results

Prepared by R.B. Stonesifer, E.F. Rybicki, D.E. McCabe

Materials Engineering Associates, Inc.

Prepared for
U.S. Nuclear Regulatory
Commission

AVAILABILITY NOTICE

Availability of Reference Materials Cited in NRC Publications

Most documents cited in NRC publications will be available from one of the following sources:

1. The NRC Public Document Room, 2120 L Street, NW, Lower Level, Washington, DC 20555

2. The Superintendent of Documents, U.S. Government Printing Office, P.O. Box 37082, Washington, DC 20013-7082

3. The National Technical Information Service, Springfield, VA 22161

Although the listing that follows represents the majority of documents cited in NRC publications, it is not intended to be exhaustive.

Referenced documents available for inspection and copying for a fee from the NRC Public Document Room include NRC correspondence and internal NRC memoranda; NRC Office of Inspection and Enforcement bulletins, circulars, information notices, inspection and investigation notices; Licensee Event Reports; vendor reports and correspondence; Commission papers; and applicant and licensee documents and correspondence.

The following documents in the NUREG series are available for purchase from the GPO Sales Program: formal NRC staff and contractor reports, NRC-sponsored conference proceedings, and NRC booklets and brochures. Also available are Regulatory Guides, NRC regulations in the *Code of Federal Regulations*, and *Nuclear Regulatory Commission Issuances*.

Documents available from the National Technical Information Service include NUREG series reports and technical reports prepared by other federal agencies and reports prepared by the Atomic Energy Commission, forerunner agency to the Nuclear Regulatory Commission.

Documents available from public and special technical libraries include all open literature items, such as books, journal and periodical articles, and transactions. *Federal Register* notices, federal and state legislation, and congressional reports can usually be obtained from these libraries.

Documents such as theses, dissertations, foreign reports and translations, and non-NRC conference proceedings are available for purchase from the organization sponsoring the publication cited.

Single copies of NRC draft reports are available free, to the extent of supply, upon written request to the Office of Information Resources Management, Distribution Section, U.S. Nuclear Regulatory Commission, Washington, DC 20555.

Copies of industry codes and standards used in a substantive manner in the NRC regulatory process are maintained at the NRC Library, 7920 Norfolk Avenue, Bethesda, Maryland, and are available there for reference use by the public. Codes and standards are usually copyrighted and may be purchased from the originating organization or, if they are American National Standards, from the American National Standards Institute, 1430 Broadway, New York, NY 10018.

NUREG/CR-5208
MEA-2305
RF, R5

Warm Prestress Modeling: Comparison of Models and Experimental Results

Manuscript Completed: January 1989
Date Published: April 1989

Prepared by
R.B. Stonesifer*, E.F. Rybicki**, D.E. McCabe

Materials Engineering Associates, Inc.
9700-B Martin Luther King, Jr. Highway
Lanham, MD 20706-1837

*Computational Mechanics
Julian, PA 16844

**The University of Tulsa
Tulsa, OK 74104

Prepared for
Division of Engineering
Office of Nuclear Regulatory Research
U.S. Nuclear Regulatory Commission
Washington, DC 20555
NRC FIN B8900

ABSTRACT

Warm prestress (WPS) behavior is the term commonly used to describe an apparent increase in material toughness of pressure vessel steels resulting from previous loading at a higher temperature. Such load histories are of interest largely due to the fact that loss of coolant accident (LOCA) and pressurized thermal shock (PTS) related load histories are expected to result in WPS behavior. While previous experimental work has demonstrated WPS behavior, insufficient attention has been given to separating material toughness variability from the WPS effect. There also appears to be a basic lack of understanding of the mechanism by which WPS behavior occurs and as a result, there is no generally accepted model or fracture criterion for predicting WPS behavior.

The objectives of this study were to develop WPS data for which the enhanced toughness due to WPS could be separated from the K_{Ic} variability of the virgin material and to evaluate several candidate WPS models.

Two types of WPS loading sequences were considered. The first is called load-unload-cool-fail (LUCF) and the second is called load-partial unload-cool-fail (LPUCF). Each load history was replicated 8 to 10 times and statistical methods were used to show that WPS can raise the apparent K_{Ic} to levels significantly above the virgin material K_{Ic} range. The LPUCF experiments showed, for example, that the effective K_{Ic} after WPS (i.e., the applied K_I at failure or K_f) was at about the same K_I level reached during the warm preload or about three times the mean virgin material K_{Ic} at the failure temperature. For the LUCF experiments the warm prestressing benefit was smaller but still significant with K_f levels being 1.6 to 2.5 times the virgin material K_{Ic} levels depending on the temperature at failure.

The WPS models which were evaluated include the small scale yield, strip yield model of Chell and associates, the compact specimen strip yield model of Newman and Mall, and a small scale yield model proposed by Curry. The candidate fracture criteria included J_e, T^*_p, dCTOD*FLOW, and critical stress.

The small scale yield critical stress model (SSYCSM) of Curry was found to be the most promising model in terms of (i) accurately predicting WPS fracture behavior, (ii) having a sound physical basis, (iii) being easy to use, and (iv) having general applicability to a wide range of geometries and WPS load histories. Proposals are made for simplifying the determination of critical stress parameters for a given material and for improving the models representation of virgin material toughness in the transition region.

CONTENTS

LIST OF FIGURES

LIST OF FIGURES

LIST OF TABLES

FOREWORD

The work reported here was performed at Materials Engineering Associates (MEA) under the program, Structural Integrity of Water Reactor Pressure Boundary Components, F. J. Loss, Program Manager. The program is sponsored by the Office of Nuclear Regulatory Research of the U. S. Nuclear Regulatory Commission (NRC). The technical monitor for the NRC is Alfred Taboada.

Prior reports under the current contract are listed below:

1. J. R. Hawthorne, "Significance of Nickel and Copper to Radiation Sensitivity and Postirradiation Heat Treatment Recovery of Reactor Vessel Steels," USNRC Report NUREG/CR-2948, Nov. 1982.

2. "Structural Integrity of Water Reactor Pressure Boundary Components, Annual Report for 1982," F. J. Loss, Ed., USNRC Report NUREG/CR-3228, Vol. 1, Apr. 1983.

3. J. R. Hawthorne, "Exploratory Assessment of Postirradiation Heat Treatment Variables in Notch Ductility Recovery of A 533-B Steel," USNRC Report NUREG/CR-3229, Apr. 1983.

4. W. H. Cullen, K. Torronen, and M. Kemppainen, "Effects of Temperature on Fatigue Crack Growth of A 508-2 Steel in LWR Environment," USNRC Report NUREG/CR-3230, Apr. 1983.

5. "Proceedings of the International Atomic Energy Agency Specialists' Meeting on Subcritical Crack Growth," Vols. 1 and 2, W. H. Cullen, Ed., USNRC Conference Proceeding NUREG/CP-0044, May 1983.

6. W. H. Cullen, "Fatigue Crack Growth Rates of A 508-2 Steel in Pressurized, High-Temperature Water," USNRC Report NUREG/CR-3294, June 1983.

7. J. R. Hawthorne, B. H. Menke, and A. L. Hiser, "Notch Ductility and Fracture Toughness Degradation of A 302-B and A 533-B Reference Plates from PSF Simulated Surveillance and Through-Wall Irradiation Capsules," USNRC Report NUREG/CR-3295, Vol. 1, Apr. 1984.

8. J. R. Hawthorne and B. H. Menke, "Postirradiation Notch Ductility and Tensile Strength Determinations for PSF Simulated Surveillance and Through-Wall Specimen Capsules," USNRC Report NUREG/CR-3295, Vol. 2, Apr. 1984.

9. A. L. Hiser and F. J. Loss, "Alternative Procedures for J-R Curve Determination," USNRC Report NUREG/CR-3402, July 1983.

10. A. L. Hiser, F. J. Loss, and B. H. Menke, "J-R Curve Characterization of Irradiated Low Upper Shelf Welds," USNRC Report NUREG/CR-3506, Apr. 1984.

11. W. H. Cullen, R. E. Taylor, K. Torronen, and M. Kemppainen, "The Temperature Dependence of Fatigue Crack Growth Rates of A 351 CF8A Cast Stainless Steel in LWR Environment," USNRC Report NUREG/CR-3546, Apr. 1984.

12. "Structural Integrity of Light Water Reactor Pressure Boundary Components -- Four-Year Plan 1984-1988," F. J. Loss, Ed., USNRC Report NUREG/CR-3788, Sep. 1984.

13. W. H. Cullen and A. L. Hiser, "Behavior of Subcritical and Slow-Stable Crack Growth Following a Postirradiation Thermal Anneal Cycle," USNRC Report NUREG/CR-3833, Aug. 1984.

14. "Structural Integrity of Water Reactor Pressure Boundary Components: Annual Report for 1983," F. J. Loss, Ed., USNRC Report NUREG/CR-3228, Vol. 2, Sept. 1984.

15. W. H. Cullen, "Fatigue Crack Growth Rates of Low-Carbon and Stainless Piping Steels in PWR Environment," USNRC Report NUREG/CR-3945, Feb. 1985.

16. W. H. Cullen, M. Kemppainen, H. Hanninen, and K. Torronen, "The Effects of Sulfur Chemistry and Flow Rate on Fatigue Crack Growth Rates in LWR Environments," USNRC Report NUREG/CR-4121, Feb. 1985.

17. "Structural Integrity of Water Reactor Pressure Boundary Components: Annual Report for 1984," F. J. Loss, Ed., USNRC Report NUREG/CR-3228, Vol. 3, June 1985.

18. A. L. Hiser, "Correlation of C_v and K_{Ic}/K_{Jc} Transition Temperature Increases Due to Irradiation," USNRC Report NUREG/CR-4395, Nov. 1985.

19. W. H. Cullen, G. Gabetta, and H. Hanninen, "A Review of the Models and Mechanisms For Environmentally-Assisted Crack Growth of Pressure Vessel and Piping Steels in PWR Environments," USNRC Report NUREG/CR-4422, Dec. 1985.

20. "Proceedings of the Second International Atomic Energy Agency Specialists' Meeting on Subcritical Crack Growth," W. H. Cullen, Ed., USNRC Conference Proceeding NUREG/CP-0067, Vols. 1 and 2, Apr. 1986.

21. J. R. Hawthorne, "Exploratory Studies of Element Interactions and Composition Dependencies in Radiation Sensitivity Development," USNRC Report NUREG/CR-4437, Nov. 1985.

22. R. B. Stonesifer and E. F. Rybicki, "Development of Models for Warm Prestressing," USNRC Report NUREG/CR-4491, Jan. 1987.

23. E. F. Rybicki and R. B. Stonesifer, "Computational Model for Residual Stresses in a Clad Plate and Clad Fracture Specimens," USNRC Report NUREG/CR-4635, Oct. 1986.

24. D. E. McCabe, "Plan for Experimental Characterization of Vessel Steel After Irradiation," USNRC Report NUREG/CR-4636, Oct. 1986.

25. E. F. Rybicki, J. R. Shadley, and A. S. Sandhu, "Experimental Evaluation of Residual Stresses in a Weld Clad Plate and Clad Test Specimens," USNRC Report NUREG/CR-4646, Oct. 1986.

26. "Structural Integrity of Water Reactor Pressure Boundary Components: Annual Report for 1985," F. J. Loss, Ed., USNRC Report NUREG/CR-3228, Vol. 4, June 1986.

27. G. Gabetta and W. H. Cullen, "Application of a Two-Mechanism Model for Environmentally-Assisted Crack Growth," USNRC Report NUREG/CR-4723, Oct. 1986.

28. W. H. Cullen, "Fatigue Crack Growth Rates in Pressure Vessel and Piping Steels in LWR Environments," USNRC Report NUREG/CR-4724, Mar. 1987.

29. W. H. Cullen and M. R. Jolles, "Fatigue Crack Growth of Part-Through Cracks in Pressure Vessel and Piping Steels: Air Environment Results, USNRC Report NUREG/CR-4828 Oct. 1988.

30. D. E. McCabe, "Evaluation of Surface Cracks Embedded in Reactor Vessel Cladding Unirradiated Bend Specimens," USNRC Report NUREG/CR-4841, May 1987.

31. H. Hanninen, M. Vulli, and W. H. Cullen, "Surface Spectroscopy of Pressure Vessel Steel Fatigue Fracture Surface Films Formed in PWR Environments," USNRC Report NUREG/CR-4863, July 1987.

32. A. L. Hiser and G. M. Callahan, "A User's Guide to the NRC's Piping Fracture Mechanics Data Base (PIFRAC)," USNRC Report NUREG/CR-4894, May 1987.

33. "Proceedings of the Second CSNI Workshop on Ductile Fracture Test Methods (Paris, France, April 17-19, 1985)," F. J. Loss, Ed., USNRC Conference Proceeding NUREG/CP-0064, Aug, 1988.

34. W. H. Cullen and D. Broek, "The Effects of Variable Amplitude Loading on A 533-B Steel in High-Temperature Air and Reactor Water Environments," USNRC Report NUREG/CR-4929, April 1989.

35. "Structural Integrity of Water Reactor Pressure Boundary Components: Annual Report for 1986," F. J. Loss, Ed., USNRC Report NUREG/CR-3228, Vol. 5, July 1987.

36. F. Ebrahimi et al., "Development of a Mechanistic Understanding of Radiation Embrittlement in Reactor Pressure Vessel Steels: Final Report," USNRC Report NUREG/CR-5063, Jan. 1988.

37. J. B. Terrell, "Fatigue Life Characterization of Smooth and Notched Piping Steel Specimens in 288°C Air Environments," USNRC Report NUREG/CR-5013, May 1988.

38. A. L. Hiser, "Tensile and J-R Curve Characterization of Thermally Aged Cast Stainless Steels," USNRC Report NUREG/CR-5024, Sept. 1988.

39. J. B. Terrell, "Fatigue Strength of Smooth and Notched Specimens of ASME SA 106-B Steel in PWR Environments," USNRC Report NUREG/CR-5136, Sept. 1988.

40. D. E. McCabe, "Fracture Evaluation of Surface Cracks Embedded in Reactor Vessel Cladding: Material Property Evaluations," USNRC Report NUREG/CR-5207, Sept. 1988.

41. J. R. Hawthorne and A. L. Hiser, "Experimental Assessments of Gundremmingen RPV Archive Material for Fluence Rate Effects Studies," USNRC Report NUREG/CR-5201, Oct, 1988.

42. J. B. Terrell, "Fatigue Strength of ASME SA 106-B Welded Steel Pipes in 288°C Air Environments," USNRC Report NUREG/CR-5195, Dec. 1988.

43. A. L. Hiser, "Post-Irradiation Fracture Toughness Characterization of Four Lab-Melt Plates," USNRC Report NUREG/CR-5216, April 1989.

Prior reports dealing with the specific topic of this report are listed below:

1. R. B. Stonesifer and E. F. Rybicki, "Development of Models for Warm Prestressing," under contract to Materials Engineering Associates, Inc., report prepared for USNRC, NUREG/CR-4491, MEA-2122, June 1986.

2. F. J. Loss, R. A. Gray, Jr. and J. R. Hawthorne, "Significance of Warm Prestress to Crack Initiation During Thermal Shock," USNRL Report NRL-8165, September 29, 1977.

3. F. J. Loss, R. A. Gray, Jr. and J. R. Hawthorne, "Investigation of Warm Prestress for the Case of Small Delta T During a Reactor Loss-of-Coolant Accident," USNRL Report NRL-8198, March 9, 1978.

ACKNOWLEDGMENT

The authors gratefully acknowledge the suggestions and support of this work by Messieurs M. Vagins and A. Taboada of NRC.

EXECUTIVE SUMMARY

Warm prestressing (WPS) behavior is the term commonly used to describe an apparent increase in toughness of pressure vessel steels resulting from a previous loading at a higher temperature.

Currently, design and analysis of toughness critical conditions from loss of coolant accidents (LOCA's) and/or pressurized thermal shock (PTS) does not account for the beneficial effects of WPS. Specifically, there has been a lack of conclusive experimental testing, a lack of understanding of the basic mechanism, and a lack of a validated predictive WPS model. Before WPS effects can be accounted for in the analysis of LOCA or PTS conditions, there is a need to (1) obtain an appropriate data base, (2) identify the mechanisms and (3) develop a model to predict WPS behavior.

In a previous task (Ref. 1), the feasibility of predicting warm prestress behavior using simple analytical models was examined. In that study, WPS data were obtained from reports and papers available in the literature. While the available data qualitatively described WPS effects, a more definitive data base was needed to quantify the WPS effect and to evaluate candidate models for predicting WPS behavior. The recommendations of Reference 1 included a series of experiments with emphasis on replication of tests to separate WPS effects from the variation in K_{Ic}.

This study had two tasks. The first was to develop additional WPS data which would allow the enhanced toughness effect of WPS to be separated from the K_{Ic} variability. The second task was to evaluate several WPS models and fracture criteria by using each candidate model to predict the results of the experiments.

Two types of WPS loading conditions were considered in the experiments and in the evaluation of the WPS models. The first WPS loading is called load-unload-cool-failure (LUCF) as shown in Fig. 1 the path O-A-O-B-D. The second WPS sequence is described by load-partial unload-cool-failure (LPUCF). The partial unloading sequence is believed to more closely represent PTS conditions.

Table 1 briefly describes and comments on the candidate analytical models which were evaluated in this study. The ordering of the models is intended to reflect the relative merit of the models.

The following summarize the major results, observations and conclusions from this study.

- Data for the LUCF tests showed an average apparent increase in toughness of 150% (compared to the K_{Ic}) at the -95.5°C failure temperature, and 65% at the failure temperature of -23.3°C.

- Data for the LPUCF load history showed a more beneficial WPS effect than the LUCF history. The LPUCF data

exhibited an apparent toughness that was 205% higher than the K_{Ic} values at the failure temperature of -95.5°C.

- Analytical modeling of both the LUCF and LPUCF experiments suggested that the most promising model for predicting WPS behavior is the small scale yield, critical stress model (SSYCSM). Failure is predicted by the SSYCSM when the stress at a certain distance ahead of the crack tip reaches a critical value. Table 1 compares the SSYCSM (Model 1) to the various other models considered in this study.

- The SSYCSM has some disadvantages in its current form. Recommendations are provided to overcome these disadvantages.

- There is a need for an enlarged data base including tests with temperature-unloading histories which more closely simulate service conditions. Subcomponent tests and full scale tests are also needed. It is also necessary to demonstrate a capability for predicting WPS behavior for these more realistic conditions using a simple model.

- Tests using irradiated material are recommended as the best means to verify applicability of WPS test results. To be most conclusive, WPS loading of the fracture specimens should be applied before or during irradiation.

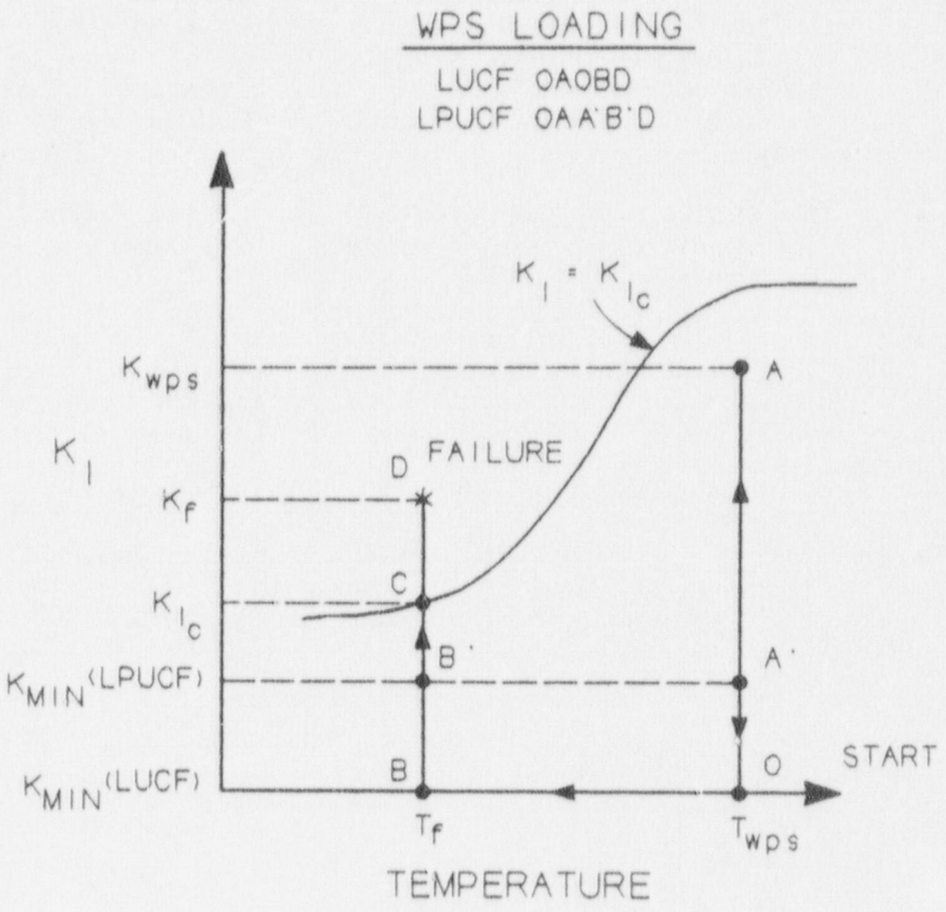

Fig. 1 Schematic representation of LUCF and LPUCF warm prestress cycles

Table 1. A Summary of the Candidate Analytical WPS Models Considered in this Study

Model	Basis for Model	Fracture Criterion	Comments
1	Superposition of small scale yield, finite element crack plane stress distributions (Refs. 7, 8 and 9)	critical stress (Refs. 18, 19, and 20)	Provides reasonable agreement with data Physical basis of critical stress criterion is clear Validity of critical stress criterion for cleavage fracture is well established Criterion can be implemented and studied via finite element modeling Critical stress is less convenient to measure than K_{Ic}
2	Superposition of small scale yield, strip yield model solutions (Refs. 4, 5, 6 and 9)	Je (Refs. 4, 10, 11 and 12)	Provides reasonable agreement with data but is less accurate than model 1 for WPS data of this study Physical basis of Je is not clear Methods for calculation of Je outside of the strip yield model (e.g. via finite elements) are not clear
3	Same as Model 2	dCTOD * FLOW (Ref. 1)	Provides reasonable agreement with data of this study but is generally found to be less accurate than models 1 and 2
4	Superposition of strip yield model solutions for a compact specimen (Refs. 26 and 27)	Je (Refs. 4, 10, 11 and 12)	Provides less accurate predictions than small scale yield, strip model though finite geometry of specimen is represented Strip yield models for specific geometries are not convenient to generate due to the need for significant amounts of numerical modeling and the difficulty of putting the numerical solutions into a form that can be efficiently used
5	Same as Model 4	dCTOD * FLOW (Ref. 1)	Same comments as for model 4
6	Same as Model 2	Tp* (Refs. 1, 16 and 17)	Exhibits behavior during cyclic loading which is opposite to that which would be required to predict WPS behavior

1. INTRODUCTION

Warm prestress (WPS) behavior is an experimentally observed phenomenon in which a material containing a flaw exhibits an apparent increase in fracture toughness due to previous loading at a higher temperature. The term WPS is associated with two types of characteristic behavior. The first and more easily understood type of WPS behavior is associated with the observed tendency for cracks to remain stable during unloading even if a material toughness decrease due to decreasing test temperature results in the applied K_I becoming larger than the material K_{Ic}. This type of WPS behavior may be applicable to loss of coolant accident (LOCA) load histories. If this applicability can be demonstrated, then WPS behavior would provide a basis for increasing calculated safety margins.

The second type of WPS behavior is also associated with simultaneous unloading and cooling but applies to the situation in which the unloading of the crack may be periodically interrupted by significant increases in the applied K_I. Experiments have shown that even in such cases, a crack can remain stable beyond the applied K_{Ic} level at which unstable growth might be expected based on the virgin material K_{Ic} range. This type of behavior may be applicable to the pressurized thermal shock (PTS) type of load history.

It can be seen that the first type of behavior is a special limiting case of the more general second type. The condition of decreasing applied K_I with time can be viewed as a sufficient (but not necessary) condition for maintaining crack stability which is in itself useful since the condition of decreasing K_I is an easily stated and easily understood criterion. Determining the necessary condition for stability under WPS loading histories of the second type requires a much more quantitative examination of the problem.

While previous experiment work has provided evidence for the existence of both types of WPS behavior, the data has not provided the type of information needed to separate WPS effects from effects of material variability in a statistical or quantitative sense. Therefore, the first task of the present study was to generate new WPS data which could be the basis for a quantitative analysis of WPS behavior. The second task was to use this new data to develop a predictive capability for fracture behavior under WPS conditions.

Since previous studies have provided a number of candidate WPS models and fracture criteria, the approach to developing a predictive capability was to first evaluate these available models and criteria. This was done by using the models and criteria to predict the results of the new WPS experiments. If one of the models and criteria could be identified as being the most promising, then any additional work would be focused toward improving that model.

1.1 Background

In the previous study (Ref. 1), several candidate WPS models and fracture parameters were identified, compared, and evaluated through

applications to WPS experiments documented in the literature (Refs. 2 and 3). These WPS experimental data were for pressure vessel materials and were obtained using three point bend specimens. The K_{wps} loading for these data was restricted to conditions for valid K_{Ic} testing. In addition to the WPS simulations using the simple models, the study of Ref. 1 included a small scale yield finite element simulation of a particular WPS experiment. Results from the simple models were further evaluated by comparison to the results of the finite element analysis.

The first model from the literature to be evaluated was the one used by Chell, Haigh, and Vitek (Ref. 4). This model was based on the superposition of dislocation model solutions such as developed by Bilby, Cottrell, and Swinden (Ref. 5). As Chell et al. note, however, the strip yield model of Dugdale (Ref. 6) is functionally equivalent to the dislocation model and can alternatively be used as the basis for their WPS model.

The second available model was that proposed by Curry (Ref. 7). Curry's approach was very similar to that of Chell et al. in that solutions for monotonic loading conditions were superimposed so as to give an approximate representation of the crack tip stress behavior due to cyclic WPS load histories. However, instead of superimposing strip yield model solutions, Curry superimposed stress distributions from the plane strain, elastic-plastic, small scale yield, finite element solutions obtained by Tracey (Ref. 8). Curry notes that the superposition methods being used by Chell et al. and by himself are consistent with Rice's (Ref. 9) earlier analysis of the stress distribution at a fatigue crack.

The fracture criterion used by Chell et al. with the strip yield or dislocation model is called J_e and is based on the work of Bilby (Ref. 10) and Miyamoto et al. (Refs. 11 and 12). The use of the letter J implys that it is related to and has the units of the J integral, attributed to the work of Eshelby (Ref. 13), Cherepanov (Ref. 14), and Rice (Ref. 15). The subscript "e" indicates that it is evaluated with only elastic components in the integrand (even when being applied to a body with plastic deformations). Chell et al. further specified that J_e (a line integral) be evaluated along a contour which encloses the currently active plastic zone. With this restriction on contours, J_e is equal to J for monotonic loading.

Another related fracture parameter was suggested in Reference 1 for use with the strip yield model of Chell et al. This parameter was called dCTOD * FLOW , defined as the change in crack tip opening displacement (CTOD) since the most recent load reversal, times the flow stress. This quantity also has the same units as J and is equal to J for monotonic loading at least in the context of strip yield models. Generally, dCTOD * FLOW is not equal to J_e once unloading occurs and neither is equal to J since J is not defined except under monotonic loading.

A third fracture parameter was also suggested for use with the WPS strip yield model of Chell et al. This parameter is T_p^*, as defined by

Atluri, Nishioka, and Nakagaki (Ref. 16), and as further studied by Brust (Ref. 17). T_p^* is defined as a contour integral, with the same integrand as J, in the limit as the contour shrinks onto the crack tip. Unlike J, however, T_p^* is well defined for incremental plasticity and cyclic loading, and, if desired, can be evaluated using path independent far field contour and volume integrals. T_p^* is equal to J for monotonic loading conditions.

Curry uses a critical stress criterion with his model (Ref. 7). With this approach, it is assumed that cleavage fracture initiates when a critical level of stress is attained at a critical distance ahead of the crack tip. Generally, both the critical stress and the critical distance are assumed to be temperature independent material properties. Experimental evidence supporting the existence of a critical stress for cleavage fracture is presented and discussed in the work of Orowan (Ref. 18), Green and Hundy (Ref. 19), Ritchie, Knott, and Rice, (Ref. 20). A disadvantage of the critical stress criterion is that the critical stress and associated critical distance are not commonly measured material properties. Some progress has been made in overcoming this disadvantage (Refs. 1, 20, 21) by obtaining these critical parameters through the combined use of small scale yield finite element solutions and commonly available fracture toughness data.

A more detailed description of the various models and fracture criteria can be found in Reference 1. Table 1 summarizes the various models and fracture criteria that were considered in the present work.

The small scale yield finite element solution from the study of Reference 1, was found to differ from the small scale yield solution obtained by Tracy (and subsequently used by Curry) by as much as 20% in the region dominated by the HRR field (Refs. 22 and 23). No conclusion was made as to the reason for this discrepancy but the use of piece-wise linear hardening as opposed to Tracey's power-law hardening, and the use of nonsingular crack tip elements as opposed to Tracey's singular elements were suggested factors. Parks (Ref. 24) and Rice and Sorensen (Ref. 25) suspect that crack tip opening displacements from Tracey's solution could be as much as 20% below the correct values, thus suggesting another possible explanation for the differences in the two solutions: if displacements are 20% below the correct values, then it would be plausible for the stresses to be 20% above the correct values.

Generally, good agreement was found between the finite element model of Reference 1 and the strip yield model in terms of CTOD, plastic zone sizes, J (during the initial loading), and T_p^* (during all phases of loading). No parameters calculated within the finite element analysis, however, were found to be physically equivalent to or comparable to J_e calculated within the strip yield model.

The small scale yield, strip yield model of Chell et al. was found in Reference 1 to predict WPS behavior reasonably well when used with the J_e parameter, or the dCTOD * FLOW parameter. T_p^* with the strip yield model was not fully evaluated in the initial study. The critical

stress model of Curry was also found to predict WPS behavior reasonably well. Insufficient duplication of experimental data prevented the separation of WPS effects from random scatter in the toughness data and one model or fracture criterion could not be selected as being clearly superior to the others.

Finally, and perhaps most importantly, it was suggested in Ref. 1 that a series of WPS experiments be conducted in which there would be sufficient duplication of tests to allow WPS effects to be clearly separated from variability in transition temperature region toughness.

1.2 Objectives

The first objective of the present study was to generate new WPS experimental data with emphasis on defining normal data scatter for K_{Ic} and post warm prestress fracture toughness, K_f, while at the same time selecting WPS load histories which are relevant to LOCA and/or PTS conditions.

The second objective was to further evaluate and rank the candidate analytical models and fracture criteria by using them to predict failure loads for the new WPS experiments. The models to be examined included the Chell et al. small scale yield, strip yield model, dCTOD * FLOW, and T_p^* fracture criteria and the Curry small scale yield, critical stress model (SSYCSM). In addition to the above, a strip yield model, modified specifically for compact specimens by Newman and Mall (Refs. 26 and 27), was evaluated. This model obviated the problems associated with applying a small scale yield, strip yield model to a finite geometry. The ranking of the various models and criteria were made based on accuracy of predicted failure loads, rationale for their physical basis, ease of use, and general applicability to a wide range of geometries and WPS load histories.

The third and final objective was to identify and evaluate modifications, extensions, and/or generalizations to the candidate models for improving their accuracy or general usefulness.

2. EXPERIMENTAL PROGRAM

2.1 Material and Properties

The material selected was a heat of A 533-B steel (V49) especially chosen for uniformity of fracture toughness properties. The available fracture toughness data on this material was, however, in the form of Dynamic Tear Test values rather than in the preferred form of a K_{Ic} transition curve. In order to predict the proper test temperature, for the present material, data were obtained from another heat of A 533-B (W7) for which both K_{Ic} and Dynamic Tear data were available. This information was then used to infer the K_{Ic} transition of the present heat (See Fig. 2). It was estimated that the V49 virgin material K_{Ic} would be 110 MPa$\sqrt{m}$ at -23°C and 55 MPa$\sqrt{m}$ at -95°C. The K_{Ic} values subsequently determined gave reasonable confirmation with average values of 124 MPa$\sqrt{m}$ at -23°C and 68 MPa$\sqrt{m}$ at -95°C. Other mechanical properties of interest are also reported in Fig. 2.

2.2 Warm Prestress Testing

It is quite common to find WPS data on A 533-B available in the literature. However, most investigators have generally limited the magnitude of the applied K_{wps} (see Fig. 1 for definitions of K_{wps}, K_f, K_{min}) levels to satisfy validity requirements for K_{Ic} testing. For A 533-B test specimens of typical dimensions, this severely limited the magnitude of K_{wps}, and consequently the magnitude of the resultant warm prestress effect. Hence K_f values obtained subsequent to WPS oftentimes fell within the scatter band of K_{Ic} for the virgin material. Also, there was seldom sufficient replication of tests to establish a firm basis for the implied WPS effect.

The experimental plan here was designed to simulate the high K_{wps} levels and temperature excursions relevant to pressurized thermal shock (PTS) scenarios. Warm prestress was performed at 177°C (350°F); clearly on the upper shelf for the A 533-B steel chosen. To demonstrate warm prestress principles, it would be necessary only to warm prestress at a temperature high enough to be on the upper shelf; 49°C being sufficient in this case. (This temperature is equivalent to NDT + 120°F where NDT is the nil-ductility transition temperature defined by ASTM E 208; (NDT + 120°F is synonymous with upper shelf behavior for many structural steels.) However, 177°C was chosen because it was closer to an expected vessel wall temperature during the pressurized thermal shock scenario.

Temperatures chosen for loading to fracture were -23°C [NDT -10°F], which is in the middle to low end of the transition range, and -95.5°C, which is well into low shelf behavior. The worst case assumption on vessel wall temperature during a PTS scenario would almost certainly be in the mid-transition range and hence -23°C was expected to be more relevent to service conditions. LUCF cycles were used on approximately 2/3 of the specimens of this study. As will be shown below, WPS load cycles which involve complete unloading, result in less WPS benefit than those that involve partial unloading.

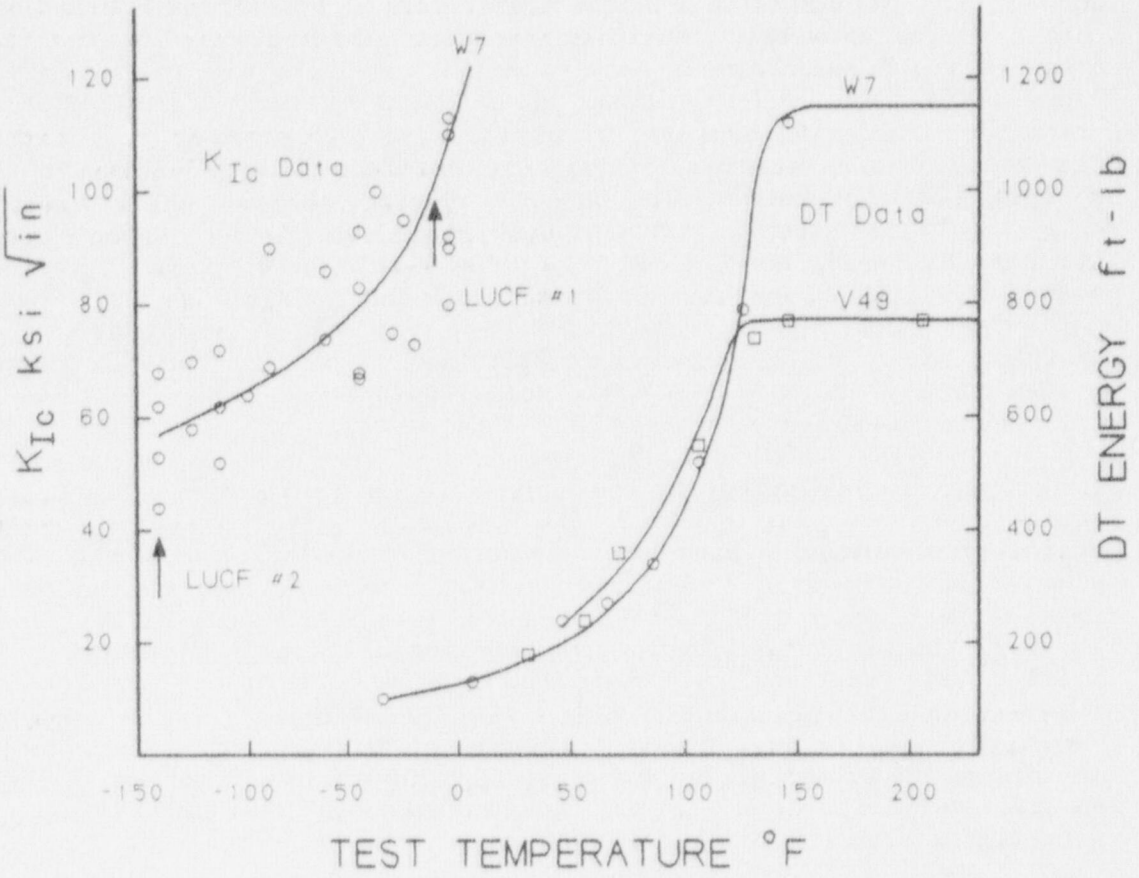

ksi $\sqrt{in}$ x 1.1 = MPa $\sqrt{m}$
ft-lb x 13.7 = J

TENSILE PROPERTIES & NDT OF HEAT W7 AND V49

	Yield Strength MPa (ksi)	Tensile Strength MPa (ksi)	Percent Elongation	RT_{NDT} °F	RT_{NDT} °C	CVN @ 10°C (50°F) J	CVN @ 10°C (50°F) ft-lb
W7	498 (72.1)	640 (92.9)	23	-40	-40	82	61
V49	446 (64.7)	631 (91.6)	30.6	0	-18		

Fig. 2 Fracture toughness data from Heat W7 used to imply K_{Ic} transition temperature curve of heat V49.

Therefore, LUCF specimens should provide conservative estimates of K_f for PTS load histories which in general have only partial unloading. The failure temperature of -95.5°C (NDT -140°F) was chosen for the remainder of the LUCF specimens for two reasons: (1) to test the accuracy of the analytical models for a large range of parameters and (2) to clearly show that the warm prestress effect is not limited to a narrow range of temperature.

One K_{wps} level, 192 MPa$\sqrt{m}$ (175 ksi$\sqrt{in.}$), was used for all tests. This value is consistent with the computed WPS crack drive levels (K_I applied) commonly postulated for pressurized thermal shock scenarios. This also represents the approximate lower bound of the stress intensity factor range for onset of slow-stable crack growth (defined by J_{Ic}) in A 533-B materials under plane stress conditions:

$$K_{wps} = (JE)^{1/2} \qquad (1)$$

where E = Elastic Modulus

The 192 MPa$\sqrt{m}$ applied K_{wps}, was large enough to produce significant plasticity in the test specimens but resulted in insignificant amounts of slow-stable crack growth.

2.3 Experimental Plan Modification

The experimental plan was to employ three basic warm prestress cycles with each being replicated ten times. See Figure 3. Two were the less beneficial LUCF types (complete unloading prior to cooling) and one was a 1/3 unloading (load, partial unload, cool and fracture) LPUCF cycle.

At a later time, two of the ten LPUCF specimens were singled out to evaluate constraint effects. This change in plan was prompted by experimental K_f values which tended to exceed the predictions from the computational models. A concern was that this behavior was caused by reduced constraint, perhaps due to a specimen width/thickness ratio of 4, and therefore the two specimens were side grooved 20 percent prior to the LPUCF cycle. If the concern over constraint turned out to be unfounded, then there would be no loss in replication.

Another unintended deviation from the original test plan resulted when the pump pressure was lost during one of the LPUCF cycles, and sustained loading during cool down was lost. This specimen was removed and set aside but was then used later as an auxilliary to the LUCF study. This specimen was cooled to -110°C (-167°F) before K_f fracture.

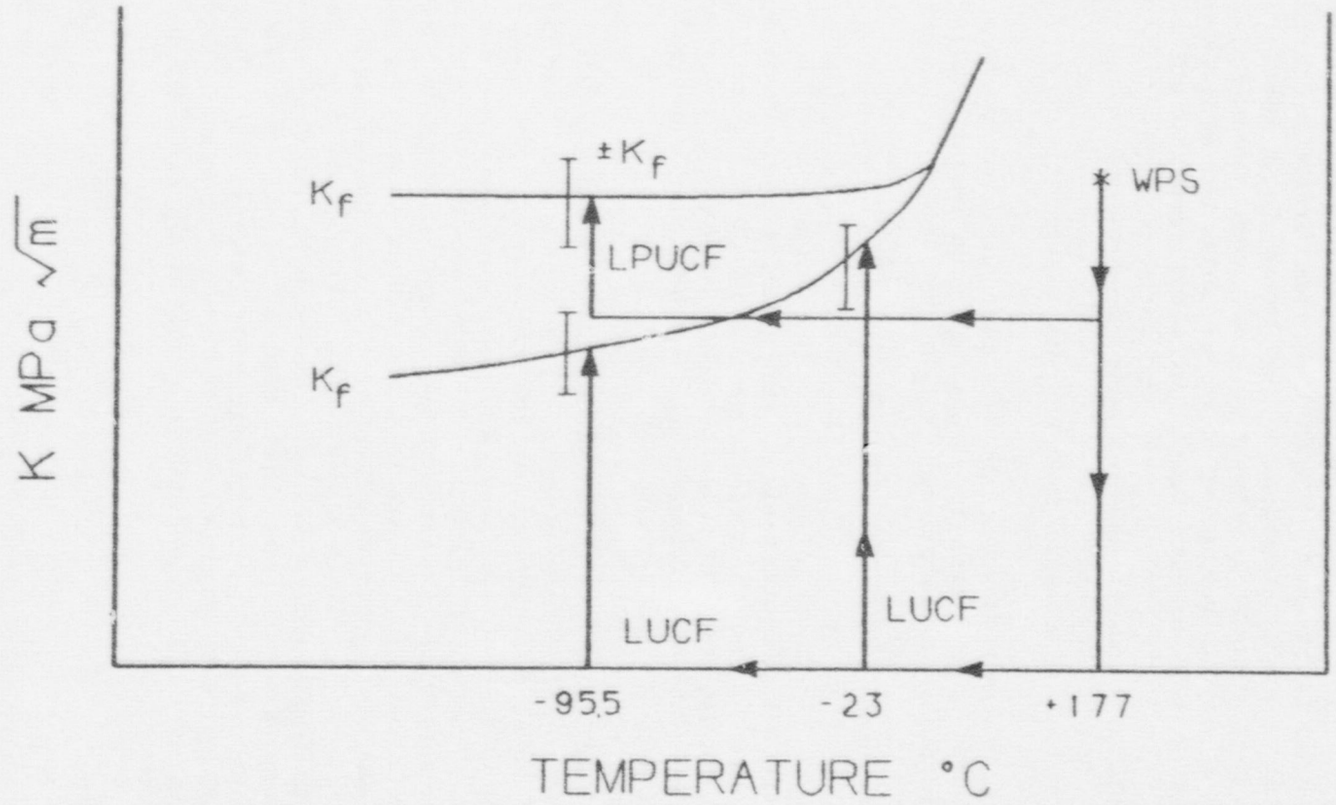

Fig. 3 Schematic of the WPS test plan of the present experiment

2.4 LUCF Testing

The test procedure is described in detail in Appendix A. A typical LUCF test record of loading at 177°C followed by unloading, cooling while at zero load, and later reloading to failure at K_f is shown in Fig. 4. Evaluation of K_{wps} was standard state-of-the-art elastic-plastic fracture mechanics since J-Integral could be accurately calculated.

K_{wps} was obtained from the experimentally measured J using Equation 1. Unlike the evaluation of K_{wps}, the calculation of an accurate applied K_f for the post warm prestress loading required development of a special analysis method. This special method was needed to account for the significant amount of plasticity resulting from the loading to K_{wps} and the residual stresses resulting from this plasticity. The method by which K_f was calculated is explained and justified in Appendix A and basically takes advantage of the fact that unloading and reloading was largely linear elastic.

The K_f values for the LUCF loading are compared to virgin material toughness in Tables 2, 3, and 4 and via Weibull two parameter statistical distributions in Figs. 5 and 6. These figures make it clear that the warm pre-stress effect is real and statistically defensible.

It will be shown in Appendix A for these tests that the WPS loading induced significant plasticity in the test specimens. As evidence of this plasticity, all of the specimens exhibited nonlinear load-deflection behavior. For the specimens of this study, unloading to zero applied load only resulted in about an 85% reduction in the effective applied K. One result of this behavior is that decreasing the external applied load to zero does not result in the effective applied K going to zero.

2.5 LPUCF Testing

Seven replicates were tested with Kwps loading followed by 1/3 partial unloading, i.e., P(sustained) = 2/3 P(wps). The partial unload level was sustained under load control during subsequent cool down to -95.5°C, after which the control mode was switched to stroke control and then the specimens were loaded to fracture at K_f. See Fig. 7. Table 5 lists individual results and Fig. 8 shows the results in the form of statistical distributions. Comparing Fig. 6 to 8, the benefit of WPS is clearly greater for LPUCF than for LUCF. In fact, the LPUCF population tends to have K_{wps} as a lower bound while the LUCF population tends to have K_{wps} as an upper bound.

The two side grooved specimens were given the identical LPUCF cycle as the non-sidegrooved specimens and both had K_f values within the scatter band of the non-side grooved specimens. See Table 5. Therefore, for all intents and purposes, there were nine replicate tests of the LPUCF type.

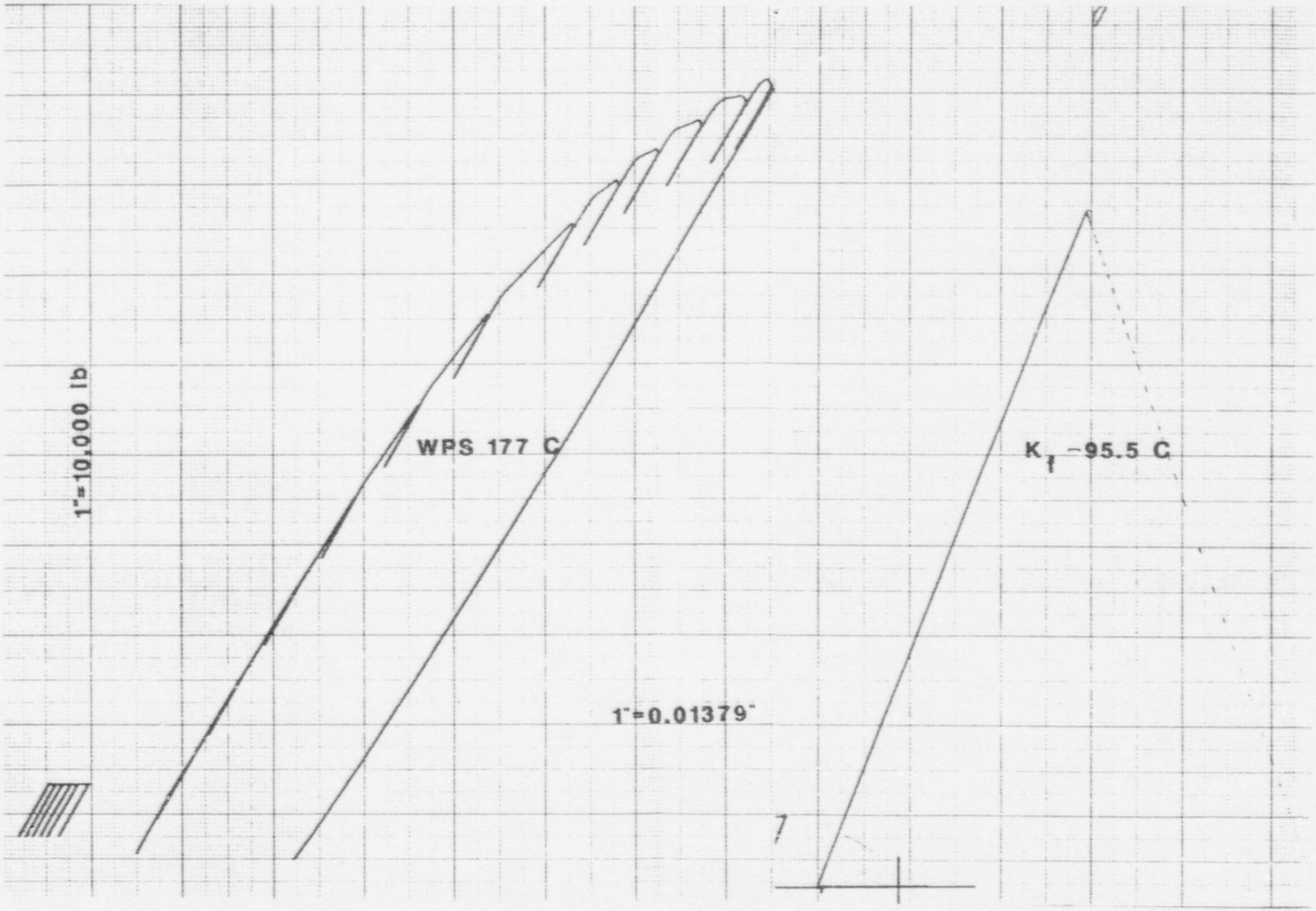

Fig. 4 Load-displacement test records for LUCF cycle.

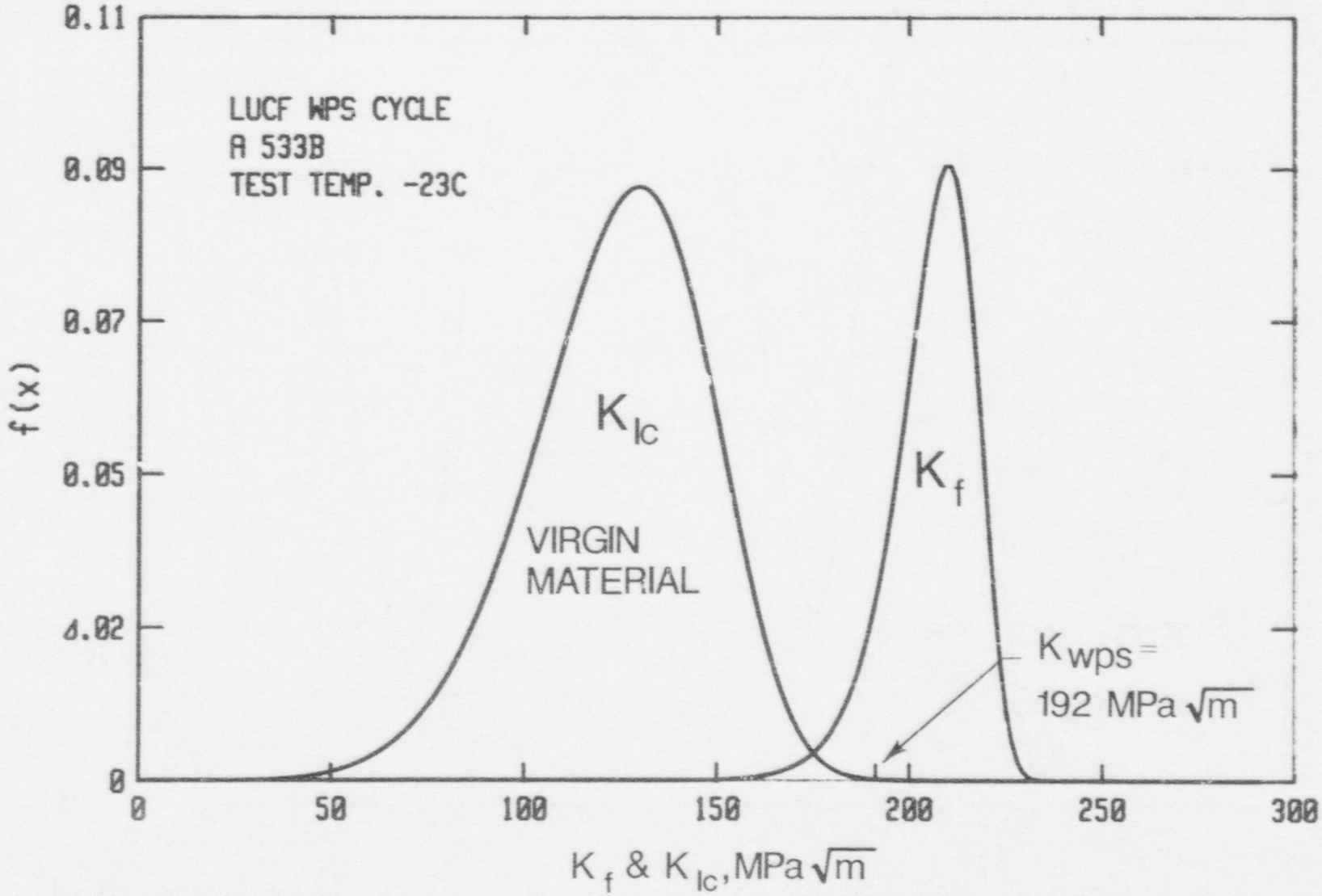

Fig. 5 K_{Ic} and K_f distribution comparison for LUCF cycle with -23°C test temperature.

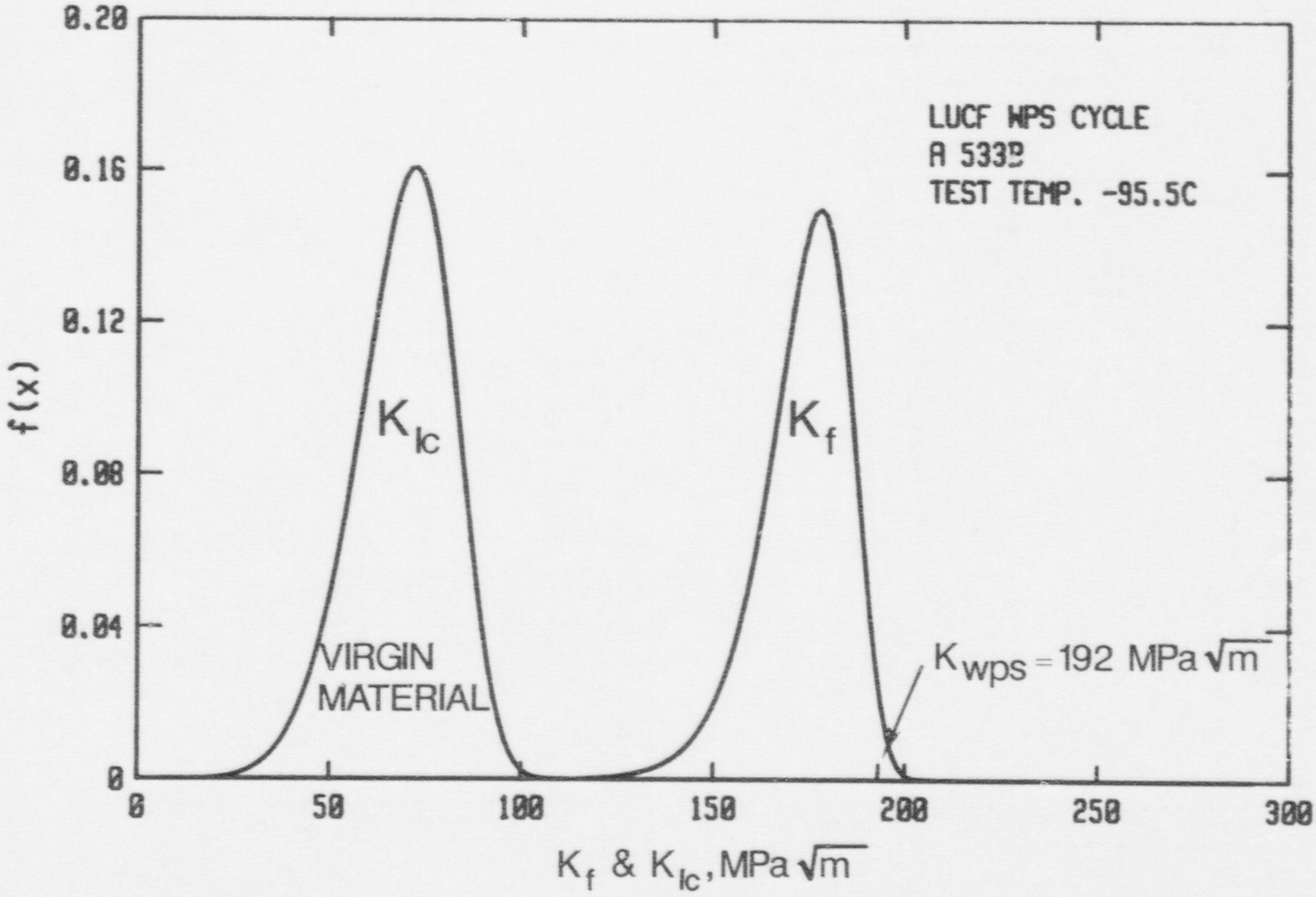

Fig. 6 K_{Ic} and K_f distribution comparison for LUCF cycle with -95.5°C test temperature.

Table 2 Material Properties (Virgin Material)

Temp. (°C)	Yield (MPa)	Tensile (MPa)	Elong. (%)	K_{Ic}[a] (MPa$\sqrt{m}$)	Std. Dev (MPa$\sqrt{m}$)
177	413	582	20.2	-	
-23	472	647	30.0	124.3	21.4
-95.5	537	739	30.3	68.3	10.4

[a] K_{Ic} Virgin Material, 1T compact specimens (25-mm thick), a/W = 0.5

Table 3 LUCF (177°C to -23°C)

K_{wps} (MPa$\sqrt{m}$)	P_{wps} (kN)	K_f (MPa$\sqrt{m}$)	P_f (kN)
190.3	391	196.7	406
192.7	404	209.6	445
195.4	379	226.2	454
191.3	375	202.0	400
192.8	401	206.8	435
199.6	412	208.5	434
196.1	397	197.1	399
195.4	409	194.9	408
196.8	383	208.7	412
195.3	408	210.6	445

Table 4 LUCF (177°C to -95.5°C)

K_{wps} (MPa$\sqrt{m}$)	P_{wps} (kN)	K_f (MPa$\sqrt{m}$)	P_f (kN)
191.8	397	169.9	344
192.2	388	187.5	376
192.[illegible]	409	177.0	372
192.1	382	159.9	303
19[illegible].6	390	184.8	374
193.8	403	169.0	343
193.1	398	158.4	315
194.8	391	182.1	360
193.1	398	181.4	369
193.4	392	167.3	329
	LUCF (177°C to -108°C)		
194.6	373	152.5	345

Table 5 LPUCF (177°C to -95.5°C)

K_{wps} (MPa$\sqrt{m}$)	P_{wps} (kN)	K_f (MPa$\sqrt{m}$)	P_f (kN)
184.7	390	196.4	418
191.6	366	215.7	424
192.6	385	219.7	452
188.7	367	214.8	429
188.9	390	213.4	450
185.4	387	202.9	429
186.7	390	210.8	448
	Side Groove 20%		
195.1	366	216.2	412
189.5	355	214.0	408

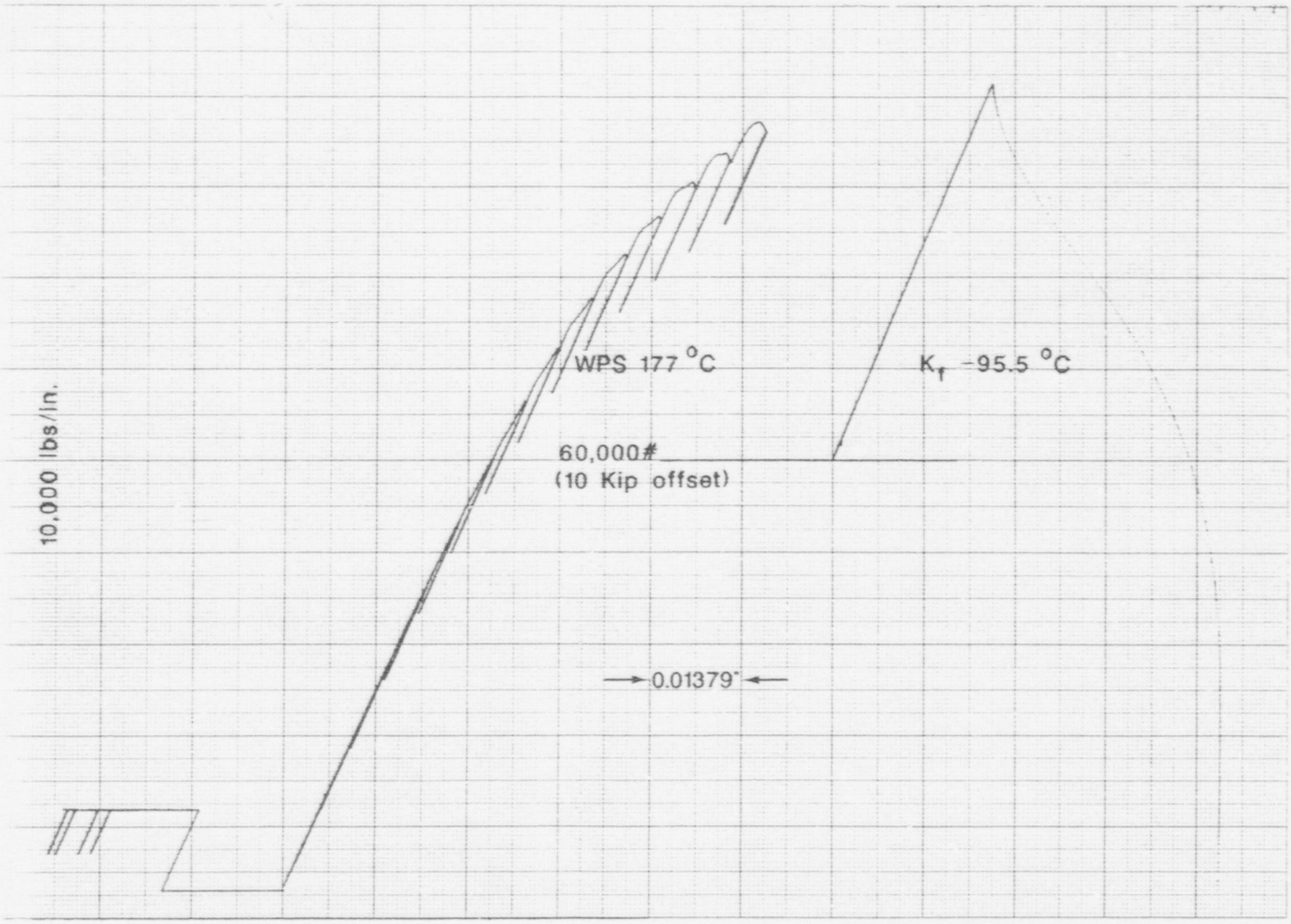

Fig. 7 Load-displacement test records for LPUCF cycle

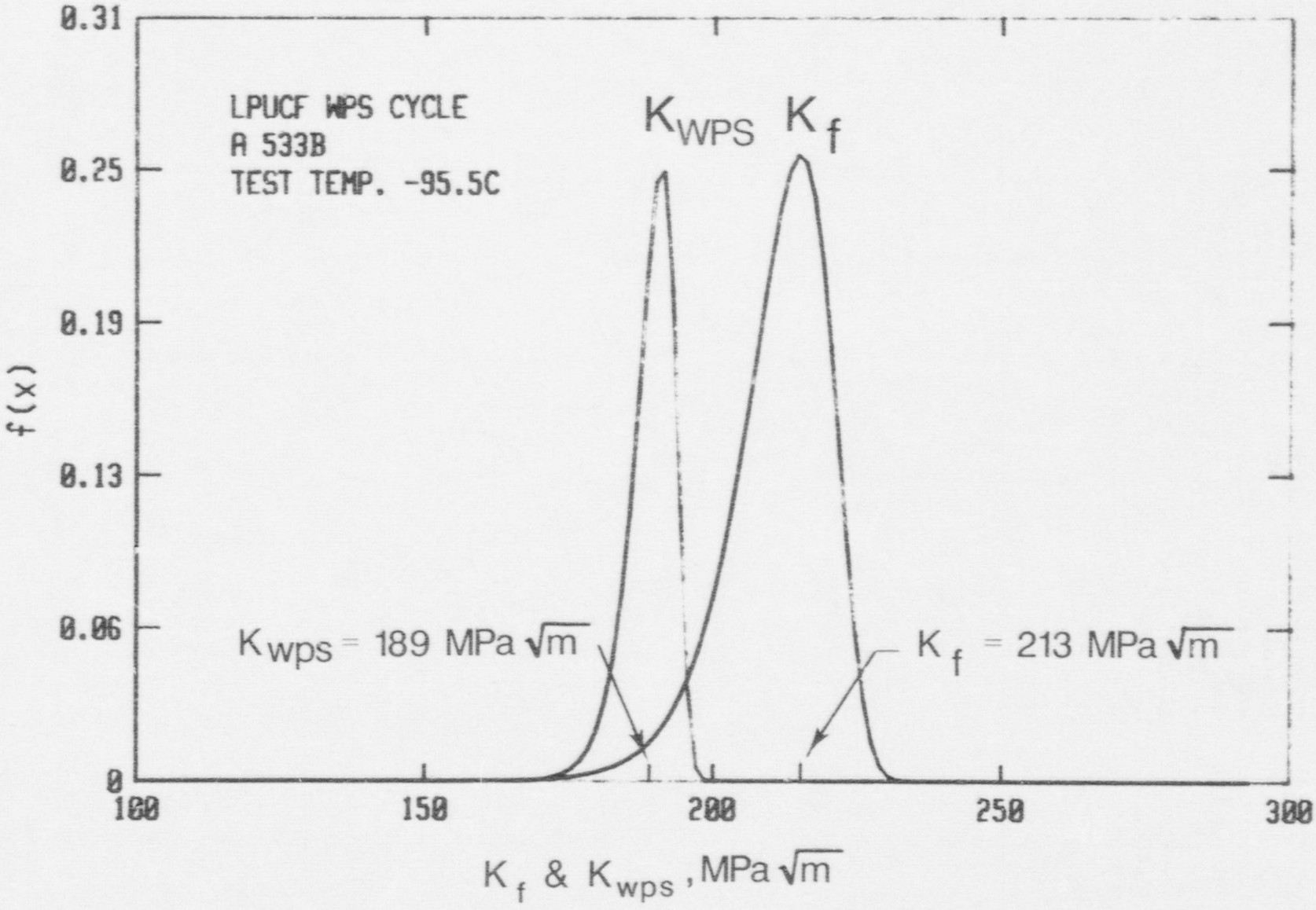

Fig. 8 Applied K_{wps} distribution and K_f distibution after LPUCF cycle down to -95.5°C. 1/3 partial unload.

2.6 Post WPS K_{Ic} Transition Temperature Curve

The LUCF and LPUCF data from this study can be used to construct K_f or effective K_{Ic} transition Curves for these two WPS load histories. Figure 9 illustrates that the fracture toughness is consistently improved by warm preloads. The present results suggest that K_f values will have K_{wps} as a lower bound if the components experience only partial unloading ($K_{min} \geq 2/3\ K_{wps}$) during a thermal transient condition. However, the extent to which this behavior is dependent on K_{wps} and the warm prestress temperature has not been addressed by the experimental program of this study.

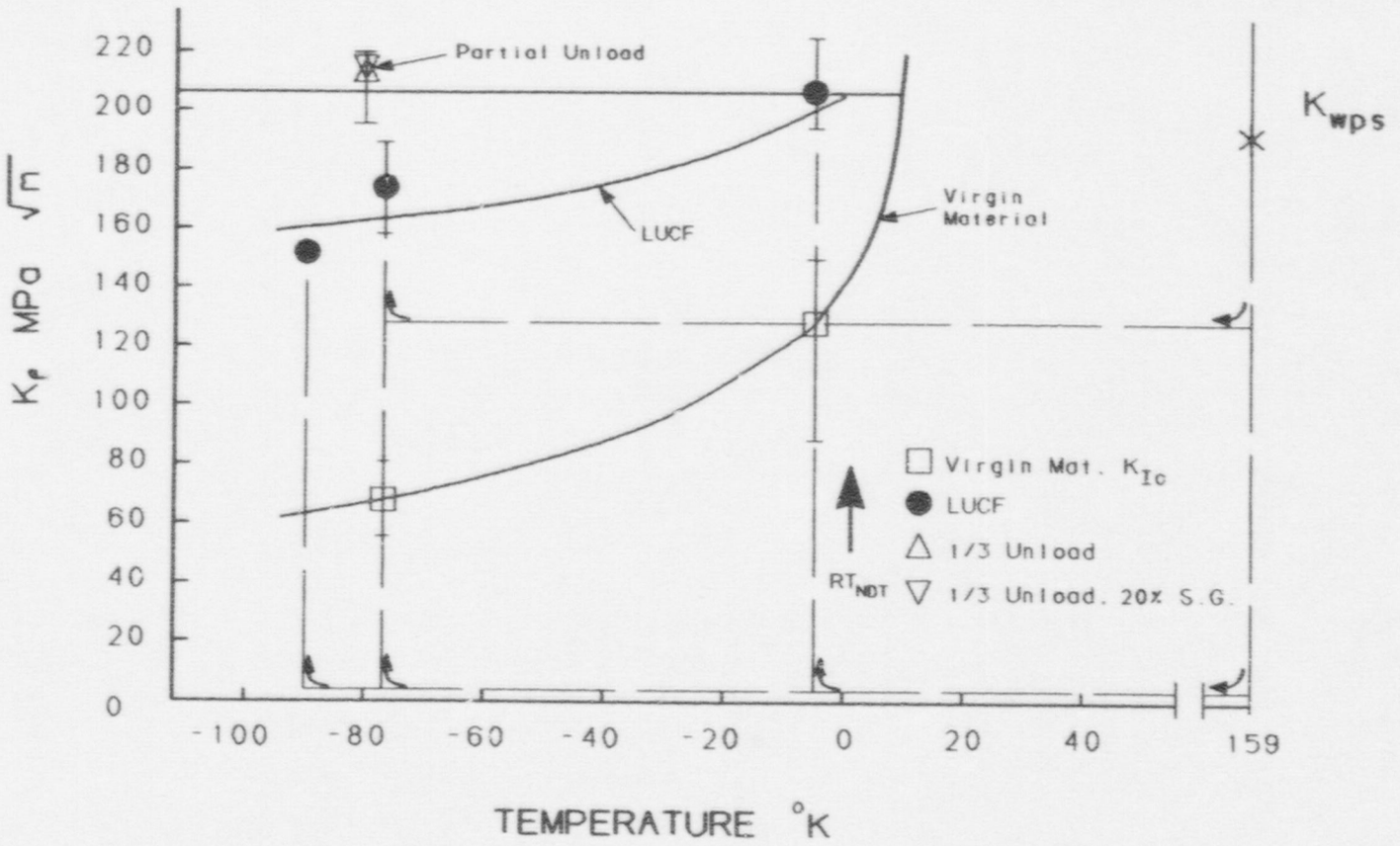

Fig. 9 Implied transition temperature shift after K_{wps} loading.

3. ANALYTICAL MODEL RESULTS AND COMPARISONS WITH DATA

This section compares and evaluates the predictions for the WPS experiments using the various candidate models and fracture criteria. It is believed that the results show that the SSYCSM offers the most promise as a simple, easy to use, physically justifiable, and yet fairly general analysis method. A further discussion of the models and further comparisons with data are provided in Appendix B.

3.1 T_p^* as a WPS Fracture Parameter

Previous finite element work on a single LUCF case (Ref. 1) suggested that failure occurred when T_p^* reached the level of T_p^* at warm prestress. Having applied this criterion to experimental data from References 2 and 3, it was subsequently observed that T_p^* often exceeds its WPS value before exceeding the fracture criterion derived from J_{Ic}, thus predicting failure for applied K levels that are less than K_{Ic}. To explain WPS behavior, just the opposite must occur. Figure 10 compares the behavior of T_p^* with that of J_e and dCTOD * FLOW (both of which have been used with some success in predicting WPS behavior). The fracture parameter during reloading must be less than its value (for a given applied load) during the initial WPS loading in order to predict typical WPS behavior.

It should be noted that within the strip yield model, dCTOD * FLOW is related to T_p^*. It can be seen from Fig. 10c that dCTOD * FLOW is equal in magnitude to the change in T_p^* since the most recent load reversal. The sign of dCTOD * FLOW during unloading can be positive or negative depending on whether FLOW is taken as a material property (always positive) or as a measure of the crack tip stress field (positive or negative depending on loading or unloading). Figure 10d also shows there is qualitative agreement between T_p^* from the strip yield model and T_p^* from the finite element model, but that significant differences exist particularly just after load reversals. Note that for the finite element model, T_p^* is defined as the limiting value as the radius of the contour (r) approaches zero.

3.2 Small Scale Yield, Strip Yield Models

Models such as the strip model are valuable tools primarily because they are simple to use relative to the more accurate finite element models. The small scale yield, strip yield model is useful for conditions where small scale yielding exists. Two disadvantages are that loading is specified in terms of a remote applied K (instead of actual applied loads) and it becomes necessary to verify that the problem of interest is indeed a small scale yielding problem.

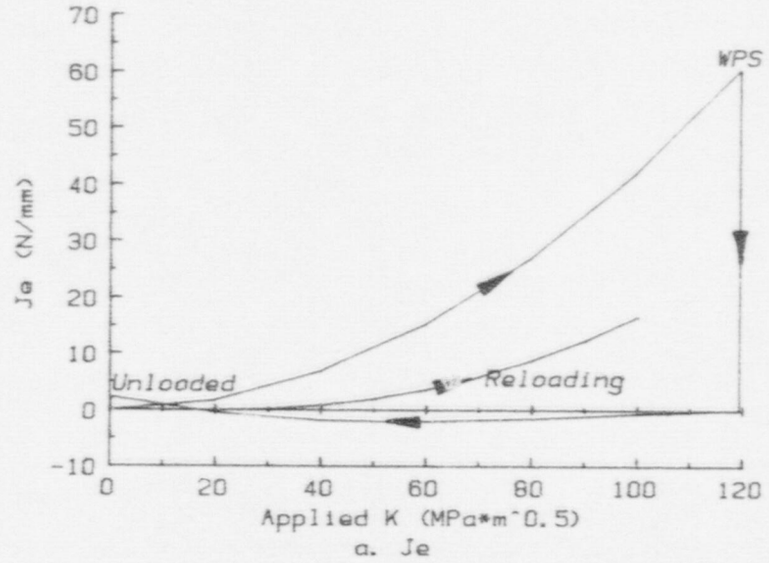

a. Je

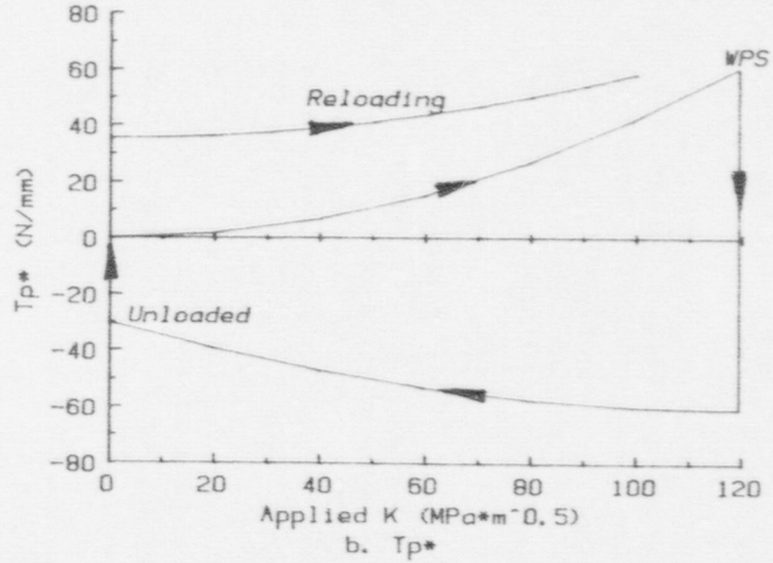

b. Tp*

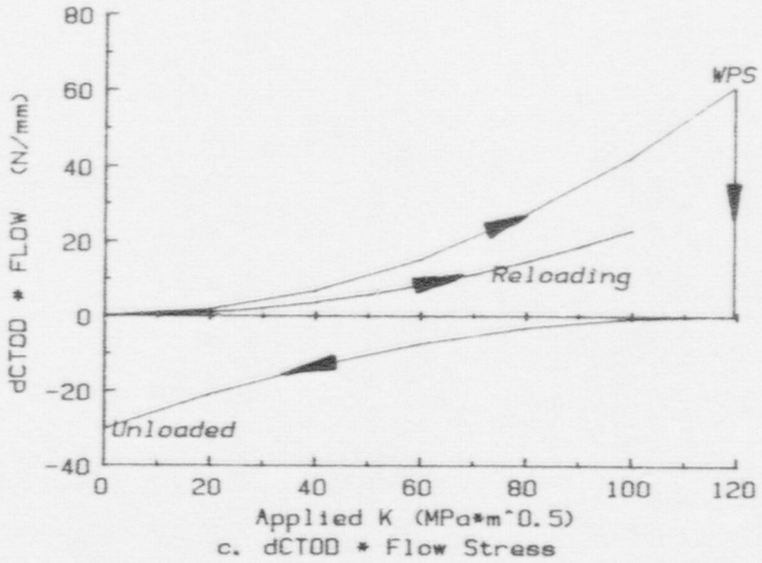

c. dCTOD * Flow Stress

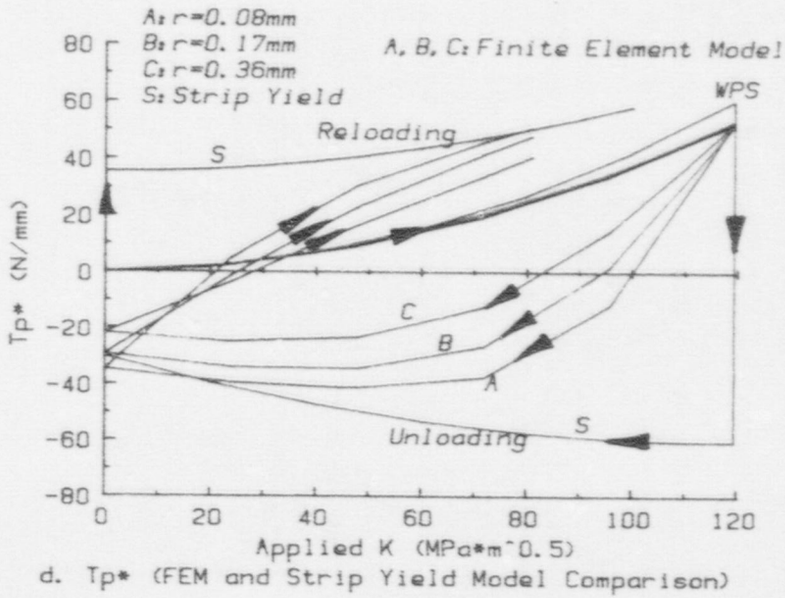

d. Tp* (FEM and Strip Yield Model Comparison)

Fig. 10 Comparison of T_p^*, Je, and dCTOD * FLOW behavior during a LUCF WPS load cycle.

3.3 Other Strip Yield Models

Newman and Mall (Refs. 26 and 27) have developed equations for a strip yield model in a compact specimen. Whereas the small scale yield, strip yield model is generally applicable to the compact specimen geometry as long as the remote load-deformation behavior is linear, the Newman and Mall model is expected to be applicable even after back face compressive yielding occurs and the load-deformation behavior becomes significantly nonlinear.

It should be noted however, that there is a significant amount of work involved in developing equations for a strip yield model for a geometry even as simple as the compact specimen. Typically, a large number of elastic finite element solutions must be obtained for two types of loading conditions and for a large range of crack sizes. Then, this information must be condensed into easy to use equations for crack opening displacements and Dugdale plastic zone sizes. Unless one is developing such equations for a geometry of general and continuing interest (e.g., a test specimen geometry) it would undoubtedly be less work to do an elastic-plastic finite element WPS analysis for the particular geometry.

3.4 Non-Small Scale Yield Considerations

The WPS experiments conducted in this study involved WPS loads which took the specimens beyond the range of small scale yielding. This is demonstrated in Fig. 11. This figure compares the postulated load vs. applied K behavior with the LEFM behavior. It can be seen that the postulated behavior (LEFM with Irwin plastic zone correction) becomes significantly nonlinear for loads above 200 kN. Similar conclusions can be made from inspection of the experimental load vs. load line displacement records. Several methods of calculating applied K from an applied load during the initial WPS loading are compared with the experimental data in Appendix A.

The difficulty that non-small scale yielding conditions introduce is in determining an appropriate relationship between the remote applied K of the small scale yield models, and the actual applied load in the experiment. For example, during unloading from the WPS load level, the K vs. load behavior would be expected to follow (for most of the unloading) the linear unloading path (DB) of Fig. 11. Unloading of 33% to 255 kN would be expected to result in an effective applied K close to that of point D, or about 136 MPa$\sqrt{m}$ (K_{min} for LPUCF cycles). For continued unloading, however, reverse plasticity at the crack tip would tend to produce a nonlinear unloading curve. If reverse plasticity was equal to the initial loading plasticity, then at zero load, one might expect the effective applied K to be near zero, point A. However, since the compressive plastic zone size due to unloading is expected to be about one quarter the size of the loading plastic zone, it is expected that the effective applied K at zero applied load will be accurately represented by point B.

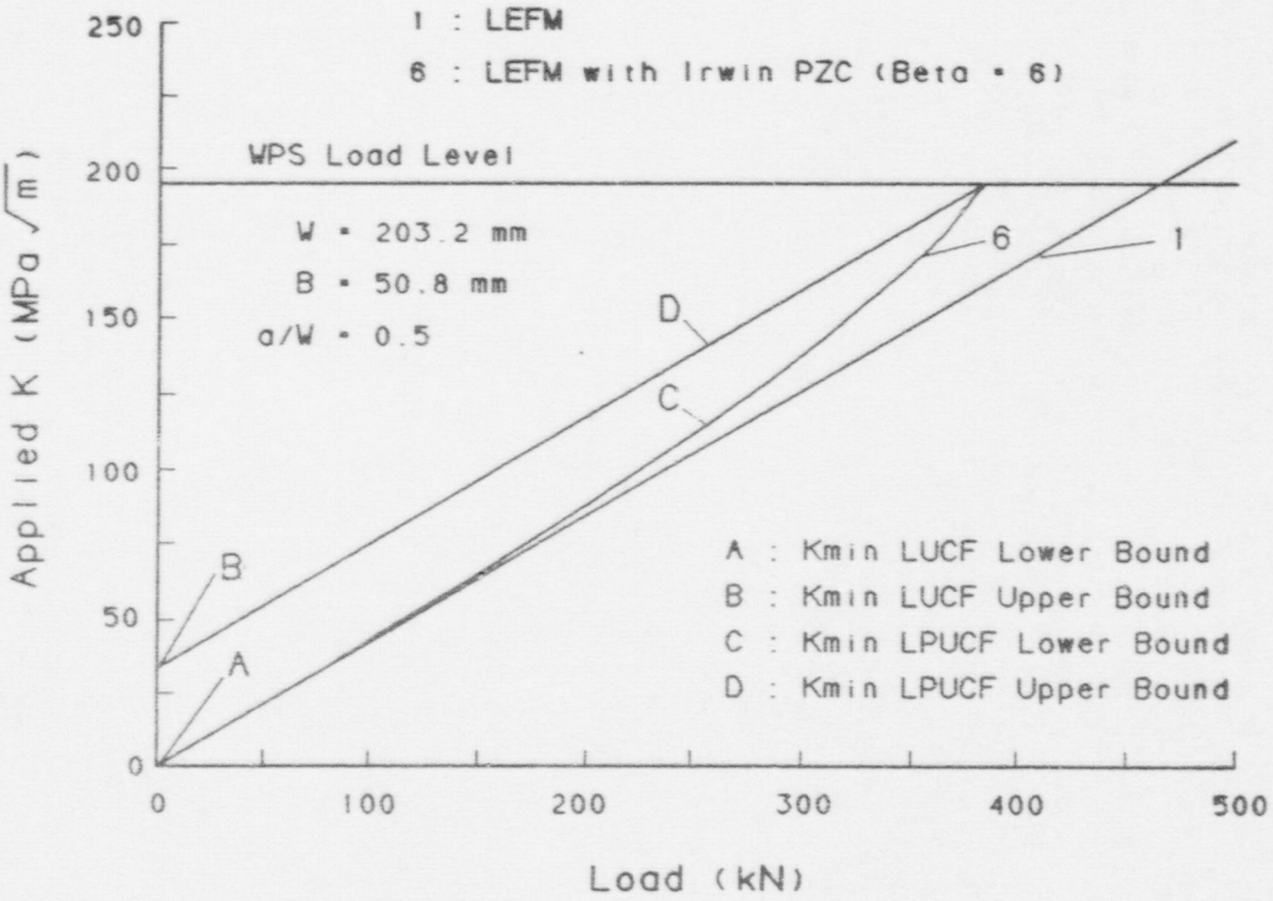

Fig. 11 The relationship between applied K and load during a WPS cycle. Path A-C WPS load. Path DB unload. Path BD reload.

Experimental load-deflection test records during unloading and reloading to failure, were essentially linear and it seems reasonable to assume that the effective applied K would also decrease and increase linearly with unloading and reloading. Therefore, experimental data points plotted in subsequent figures pertaining to small scale yield model predictions assume that the load versus effective applied K values lie on the unloading line containing points B and D in Fig. 11. The y-axis intercept of this line (K_{min} for LUCF cycles or point B) is approximately 33 MPa$\sqrt{m}$.

3.5 WPS Predictions Using J_e

The J_e criterion has been used with both the small scale yield, strip yield model and the compact specimen strip yield model. Using the small scale yield model, J_e predicted failure K values are in good agreement with the WPS data, for the LUCF history (See Fig. 12a). The largest deviation from the data is about 15% and is found at the -95.6°C failure temperature. The actual failure loads for this case are always greater than the predicted failure loads, even when using an upper bound input toughness trend. The predictions are also conservative for the LPUCF history (Fig. 13a) but to a lesser degree, predicted K_f is about 5% less than the average experimental K_f.

Due to the departure from small scale yielding in the present experiments and the resulting assumptions on applied K vs. load behavior, it was anticipated that the use of the compact specimen strip yield model of Newman and Mall would improve the J_e failure predictions for the LUCF load history. However, the predictions were found to be even less accurate (-31%),than those using the small scale yield model. See Fig. 12b. The effect of constraint was considered in this case and even though predictions were improved with added constraint, the model would not fit the LUCF experimental data. It is seen from Fig. 13 that LPUCF predictions using J_e with either strip yield model provides predictions in good agreement with the data.

One possible contributing factor for the significant sensitivity of J_e to the type of model (i.e., small scale yield strip yield vs. compact specimen strip yield) may be its dependence on deformation behavior at the remote edge of the active crack tip plastic zone. This dependence on deformations which are far removed from the crack tip is also considered to be a reason for questioning the physical basis of J_e.

3.6 WPS Predictions Using dCTOD * FLOW

The dCTOD * FLOW criterion has also been used with both the small scale yield, and the compact specimen strip yield models. Figures 14 and 15 compare dCTOD * FLOW based predictions for the LUCF and LPUCF data, respectively. Using the small scale yield model, dCTOD * FLOW predicted failure K values which are in fair agreement with the LUCF WPS data (Fig. 14a). The largest deviation from the data (-27%) was again found at the -95.6°C, failure temperature, where the actual failure loads were again greater than the predicted failure loads.

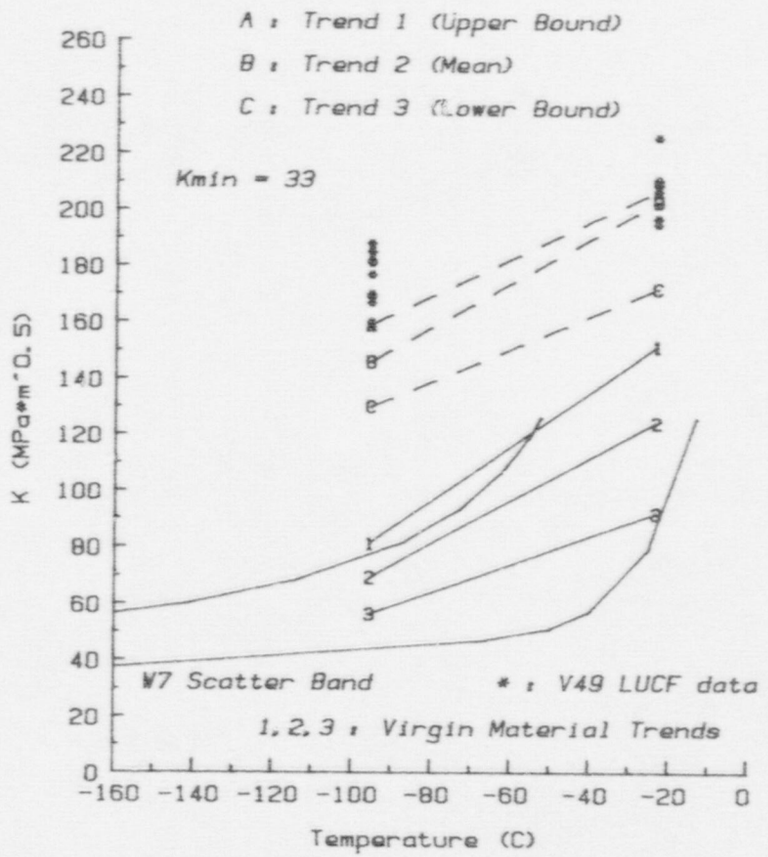

a. Je / Small Scale Yield Model

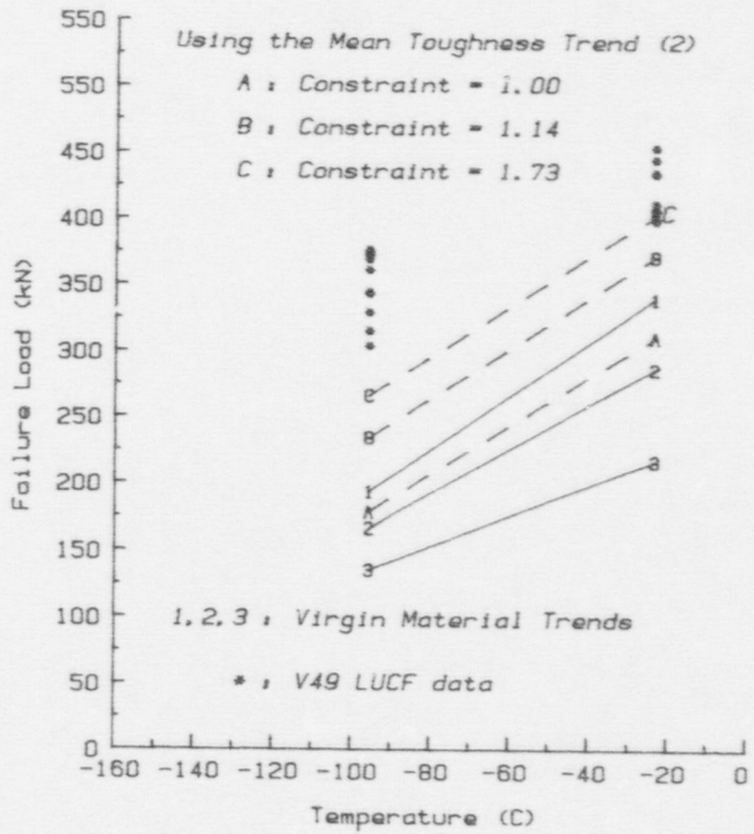

b. Je / Compact Specimen Strip Yield Model

Fig. 12 Failure predictions compared to experimental LUCF results, using J_e with small scale yield model (a), and compact specimen model (b).

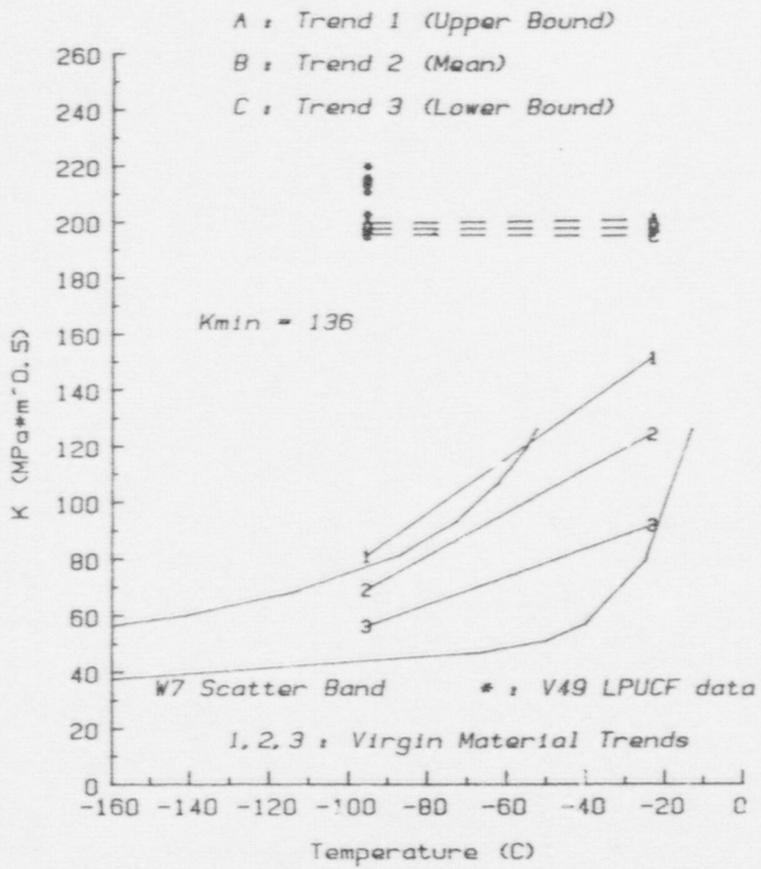

a. Je / Small Scale Yield Model

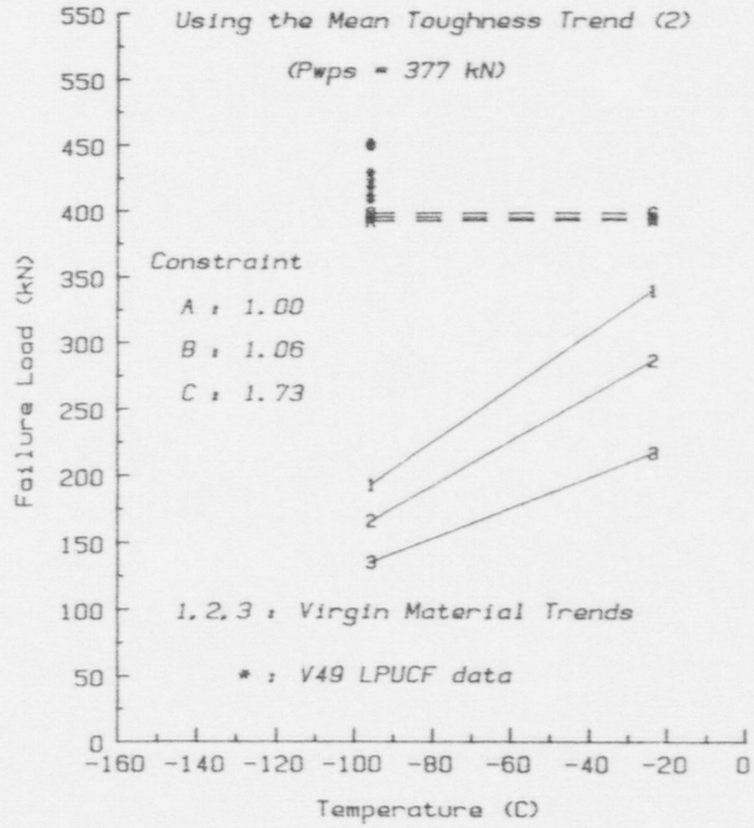

b. Je / Compact Specimen Strip Yield Model

Fig. 13 Failure predictions compared to experimental LPUCF results, using J_e with small scale yield model (a) and with compact specimen model (b).

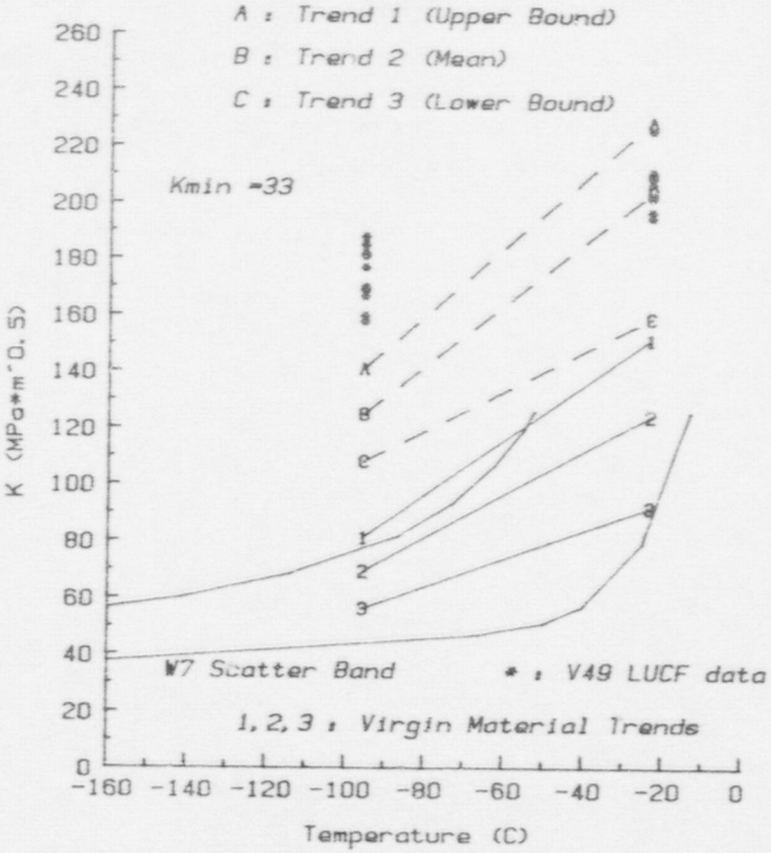

a. dCTOD * FLOW / Small Scale Yield Model

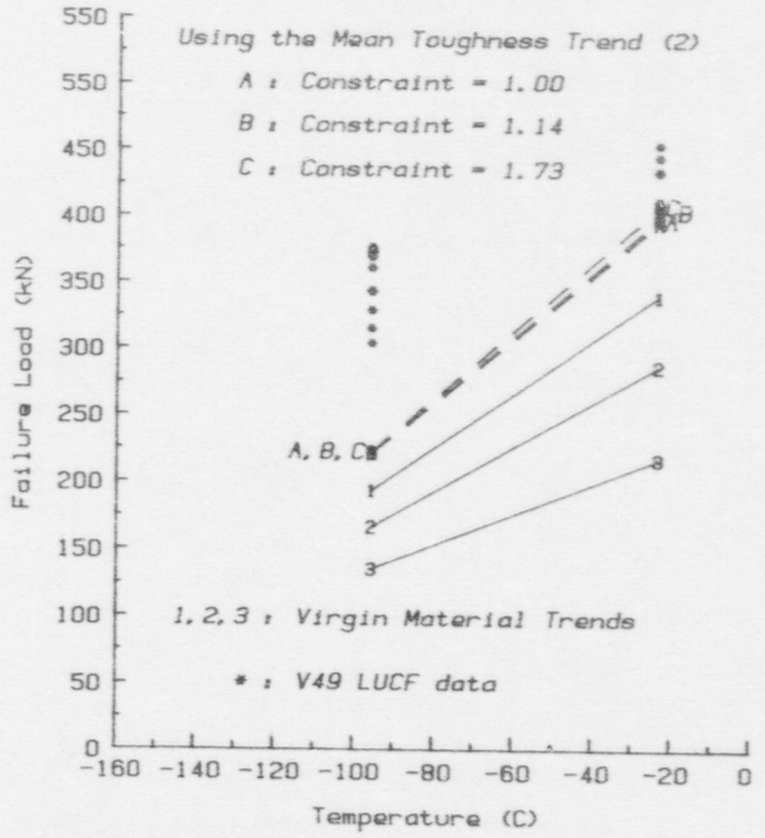

b. dCTOD * FLOW / Compact Specimen Strip Yield Model

Fig. 14 Failure predictions compared to experimental LUCF results, using dCTOD * FLOW with the small scale yield model (a), and dCTOD * FLOW with the compact specimen model (b). LUCF cycle.

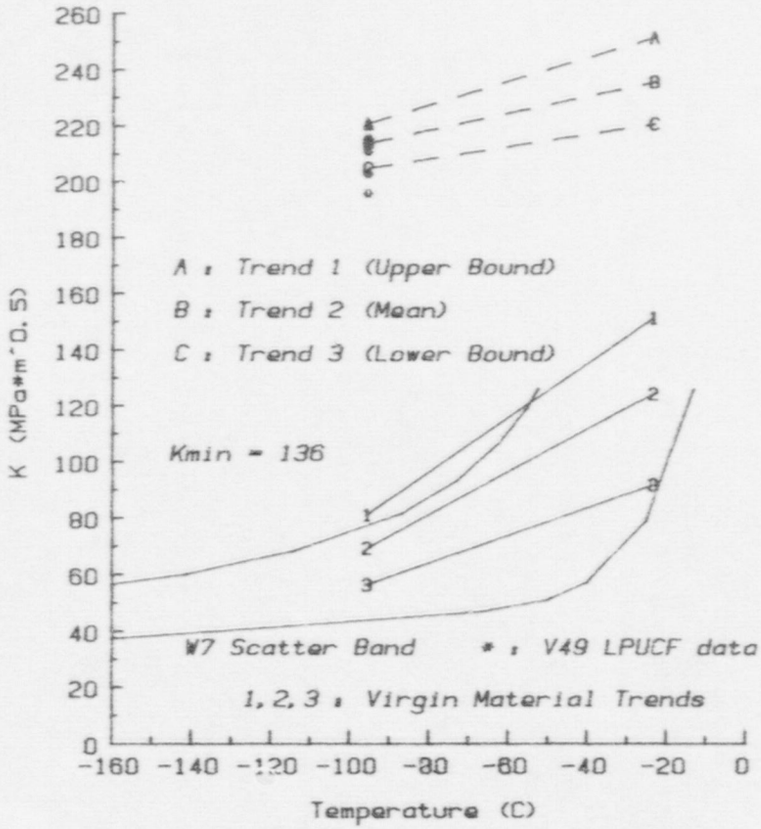

a. dCTOD * FLOW / Small Scale Yield Model

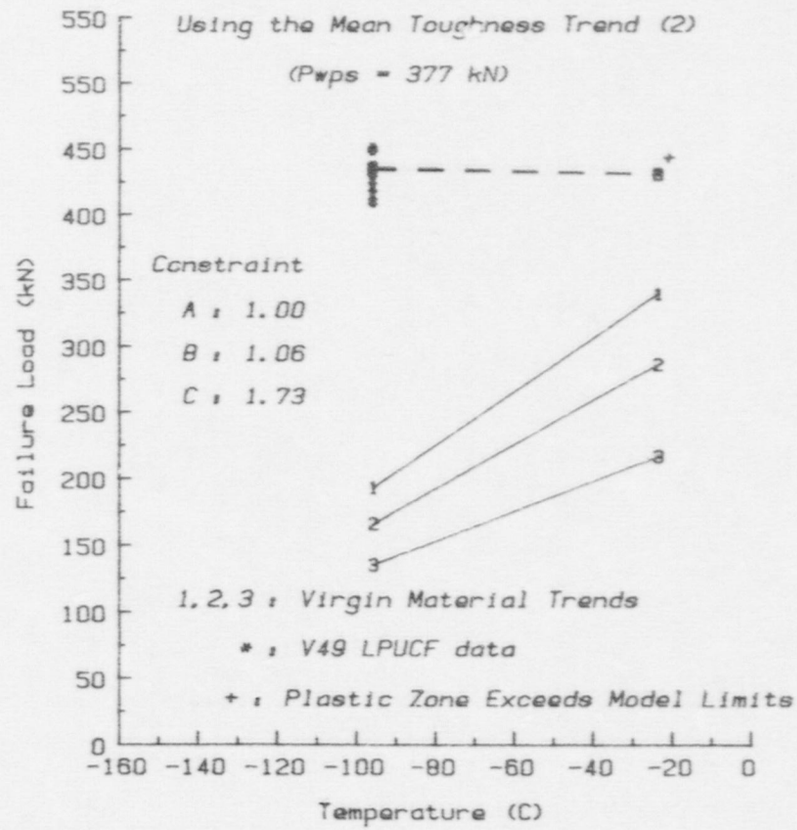

b. dCTOD * FLOW / Compact Specimen Strip Yield Model

Fig. 15 Failure predictions compared to experimental LPUCF data, using dCTOD * FLOW and small scale yield model (a), and dCTOD * FLOW with the compact specimen model (b), LPUCF cycle.

While the dCTOD * FLOW predictions at the -95.6°C failure temperature for the LUCF loading are even more conservative (less accurate) than the predictions via J_e, the dCTOD * FLOW predictions for the LPUCF history are in almost full agreement with the data, Fig. 15.

When the dCTOD * FLOW criterion was used with the compact specimen strip yield model, the predictions were again found to be less accurate (-35% for LUCF) than when using the small scale yield, strip yield model. This behavior is not to be expected if the fracture criterion is indeed a valid one. Since the compact specimen strip yield model should provide a more accurate representation of the actual specimen behavior then the small scale yield strip model, the reduced accuracy of the J_e and dCTOD * FLOW criteria tends to reduce the attractiveness of these criteria.

3.7 WPS Predictions Using Critical Stress

The use of the critical stress criterion with the superposition of small scale yield finite element solutions as suggested by Curry (SSYCSM), has the same advantages and disadvantages of being a small scale yield model as the strip yield models. A key advantage is that the model is applicable to any geometry provided that small scale yielding conditions exist. The disadvantages are that the loading must be applied to the model in terms of applied K levels, and the model cannot generally be used for non-small scale yielding conditions.

It is important to note that the small scale yield restriction is not a feature of the criterion but of the model for superposition of stress fields. The present study has shown, however, that the small scale yield restriction can be relaxed under certain conditions. (The following arguments are also applicable to the small scale yield, strip yield model.) The condition for relaxing the small scale yield restriction is that the unloading and reloading to failure results in linear load-displacement behavior at the point of the applied load i.e., small scale yielding predominates during unloading and reloading. Non-small scale yielding during the initial WPS loading is permissible as long as elastic-plastic fracture mechanics methods can be used to accurately determine the relationship between the effective applied K and the remote applied load.

Three sets of critical stress parameters (each set containing a critical stress and a critical distance) are developed in Fig. 16 for the experimentally determined virgin material toughness trends using the stress distributions of Tracey (Ref. 8). These are determined via trial and error so as to agree with the mean virgin material toughness trends for the two temperatures of interest in this study (-23.3°C and -95.6°C). A general scatter band for A 533-B is shown for perspective using the data from another heat of A 533-B reported in Reference 2.

Figure 17a compares the experimental K_f values for the LUCF WPS load history with those predicted by the SSYCSM. The effective applied K at the unloaded state (K_{min}.), for the simulation is taken as

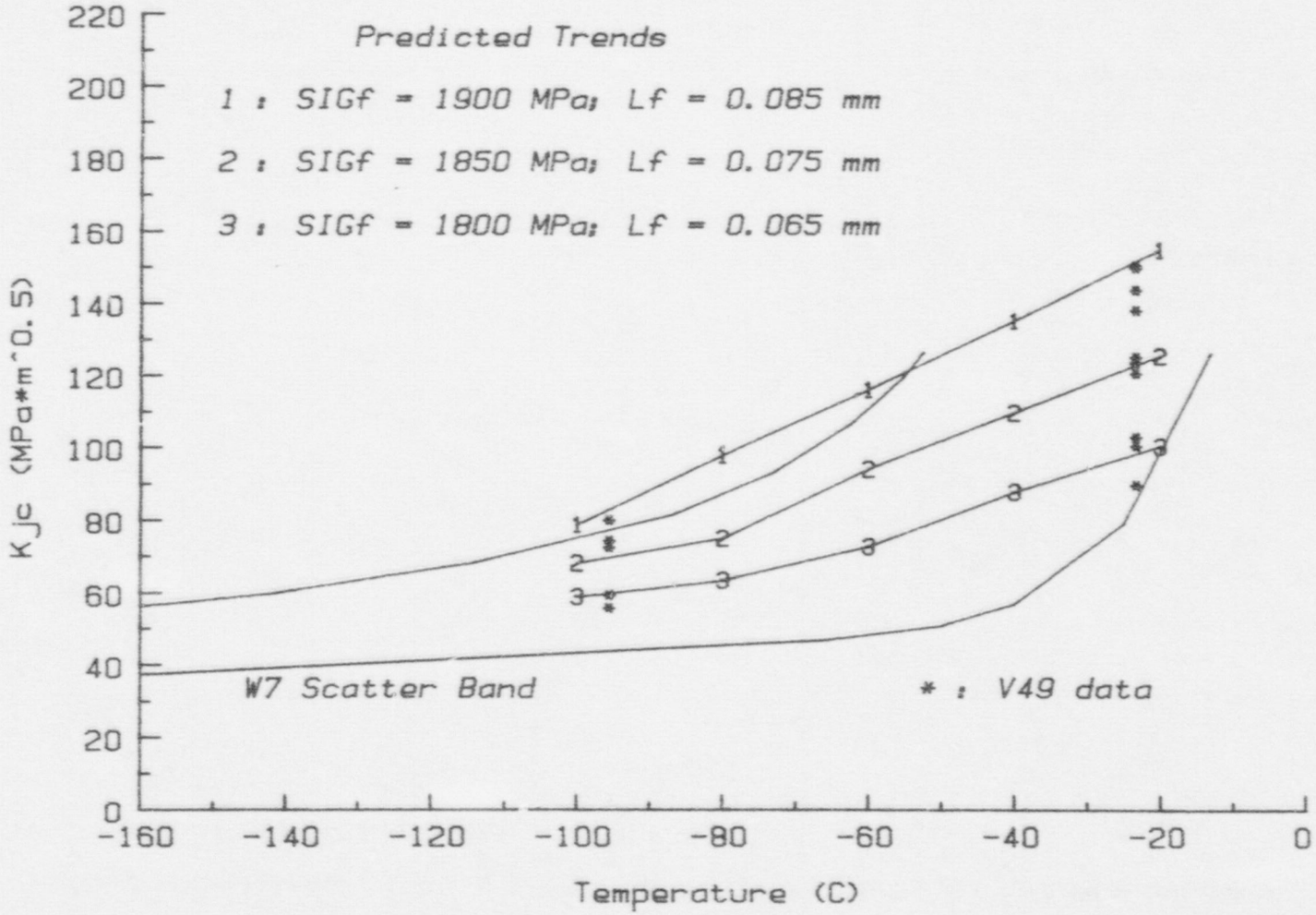

Fig. 16 Three combinations of critical stress and critical distance to fit the V49 virgin material scatter band.

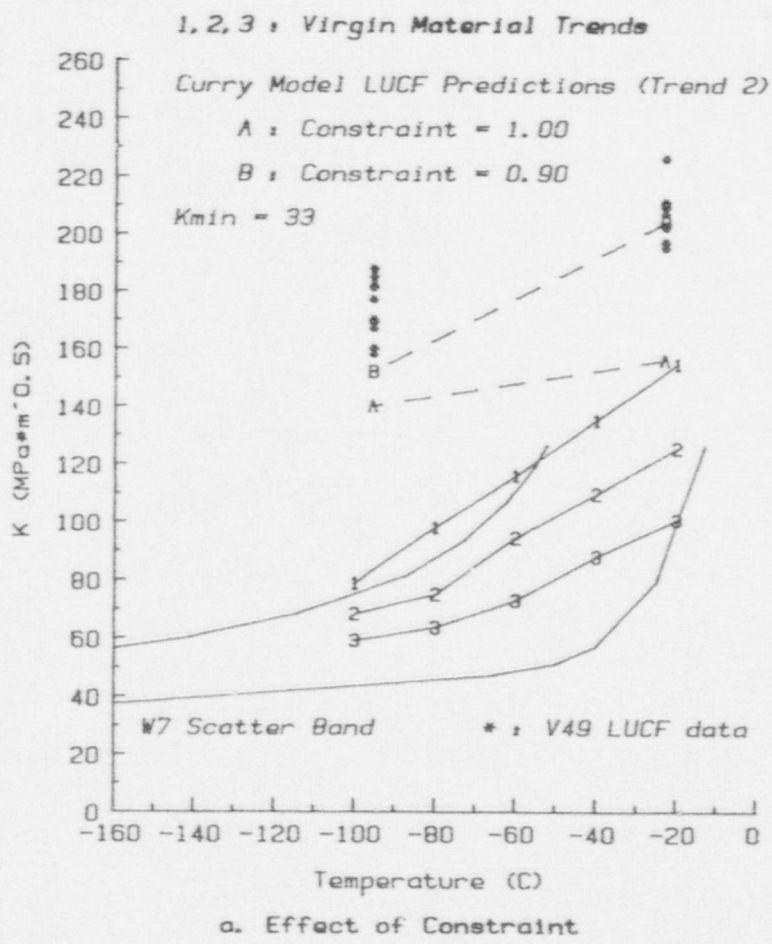

a. Effect of Constraint

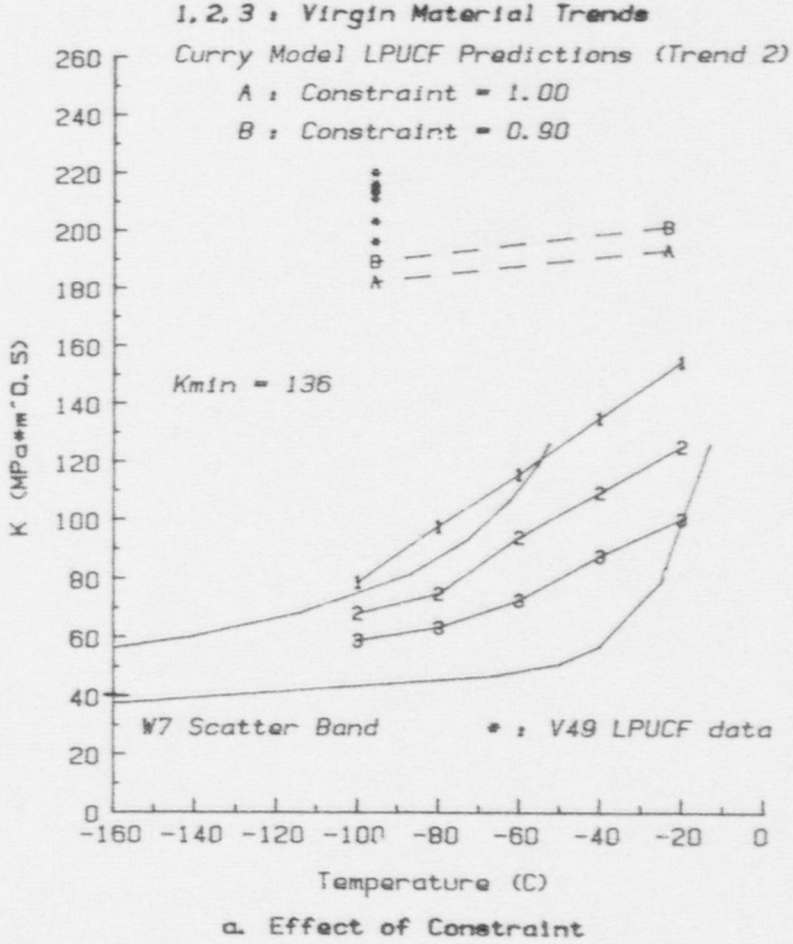

a. Effect of Constraint

Fig. 17 Comparison of predicted K_f using the SSTCSM with experimental data.

33 MPa$\sqrt{m}$ and reflects the presence of non- small scale yielding during the WPS loading, (See Appendix A). The basis for this simulation is the small scale yield stress solutions of Tracey which assumed plane strain conditions.

Experimental determination of constraint for the virgin K_{Ic} tests and the WPS tests indicated that the K_{Ic} test specimens (1T compacts, 25.4-mm thick) exibited slightly more constraint than the WPS specimens (4T compacts, 50.8-mm thick). This may have been due to the difference in specimen size or due to the thinner than standard thickness used for the WPS tests (half the standard thickness). Moderate reduction in constraint affects the WPS model by effectively reducing the yield stress. The factor of 0.9 was determined directly from the experimental constraint information on the K_{Ic} and WPS specimens, and it appears from Fig. 17 that this results in better agreement with the WPS data. This apparently high sensitivity to constraint could perhaps create some difficulty in applying the SSYCSM when information on constraint is not available. It can be seen that assuming a default constraint of unity tended to produce conservative predictions in the present study.

Figure 17b compares the experimental K_f values for the LPUCF WPS load history with those predicted by the SSYCSM. The effective applied K at the unloaded state for the simulation is taken as 136 MPa$\sqrt{m}$, again reflecting the presence of non-small scale yielding during the WPS loading. It can be seen that the model predictions are in good agreement with the experimental WPS data, although the predictions tend to be slightly conservative (-10%). Again it appears that using a lower constraint factor would tend to improve the agreement with the data.

Though failure predictions of Fig. 17 are obtained using the superposition approach of Curry and the small scale yield finite element results of Tracey, the predictions could just as well have been made via actual elastic-plastic finite element simulations of the compact specimens. While such an approach would involve significantly more computational effort, it would also remove the errors associated with superposition of nonlinear stress solutions and would eliminate the need to determine an effective applied K history since the measured loads would then be applied directly. Such an approach would also allow the critical stress criterion and the superposition model to be assessed independently.

3.8 Summary Discussion of The Critical Stress Model

While the critical stress criterion can be used with a rigorous elastic-plastic (perhaps even large deformation) finite element analysis, such a use cannot be considered simple, and probably would not be considered by many engineers for routine analysis. However, when combined with the superpositional approach of Curry within the context of small scale yielding behavior, one does indeed have an easy to use and yet widely applicable analysis tool for WPS failure analysis.

It has been shown in this study that the small scale yielding, critical stress model (SSYCSM) can be extended beyond small scale yield conditions. The actual requirement on the model is that the unloading and reloading behavior be small scale yielding; the initial WPS loading can exceed small scale yielding conditions. This extension of applicability is important since simulation of practical WPS load histories can therefore be accomplished in the laboratory using conveniently sized specimens.

An inconvenient feature of the critical stress criterion is that critical stresses are not commonly measured quantities. The experimental determination of critical stress has historically been accomplished using deeply notched bend bars. Blunted notches are used instead of cracks so that the state of stress is known, and at the same time, so that a peak stress occurs at some distance ahead of the notch root (Ref. 28, 29). While the critical stress obtained from this procedure is applicable to sharp cracks, one must still determine a critical distance which is appropriate to the sharp crack geometry. Typically, it is argued that the critical distance should be related to a microstructural dimension such as inclusion spacing or grain size, etc. (Ref. 20). Due to the uncertainty of the most appropriate microstructural dimension to be chosen, it is common to find a distance that works and then go back and see what microstructural detail the selected distance matches. Therefore, even if one goes to the trouble of determining the critical stress experimentally, using the traditional methods, one is left with choosing a critical distance in a rather ad hoc manner.

In the absence of experimental critical stress data using the above procedure, the critical stress and distance were selected in this study by trial and error so as to produce the best fit of the experimental toughness versus temperature trend (Ref. 21). The critical values determined in this way are found to be comparable to those found by others in the literature using the blunt notch experimental approach.

This trial and error approach has the added advantage that it assures the user that the WPS model will reproduce K_{Ic} results when applied to a monotonic loading problem. If the critical parameters are determined independently of K_{Ic} and the WPS model (i.e., by the direct experimental method described above) then this method can be used as an independent check.

While the trial and error approach to determining the critical stress and distance removes some of the inconvenience of using a fracture criterion other than K_{Ic}, there are still two aspects of the critical stress criterion which could bear improvement. The first is that by using the usual assumption that the critical stress and distance are temperature independent, it is not generally possible to reproduce a experimental K_{Ic} trend exactly. The second is that trial and error methods for selecting the critical parameters rely on a subjective judgement as to what constitutes a best fit of the desired K_{Ic} trend.

An approach that removes these two final inconveniences of the critical stress criterion is herein proposed. The two key features of the approach are to first allow the critical stress and critical distance to be temperature dependent, and second, assume the critical distance at a given temperature is some function of the critical CTOD at that temperature. Such an approach will make it a simple matter to determine a temperature dependent critical stress and critical distance from an input K_{Ic} versus temperature trend. It will remove the subjectivity of the trial and error fitting, and will result in an exact fit to the K_{Ic} vs. temperature trend. Since it has been found that using temperature independent values of the critical stress and distance generally provide a good fit of the K_{Ic} trend except in the transition region, it is anticipated that the critical stress and distance from such a procedure will be strongly temperature dependent only in the transition region.

3.9 Perspective on All WPS Models

While the critical stress based model has the shortcomings of requiring critical stress parameters to be specified instead of more commonly available K_{Ic} data, and not being able to represent a given virgin material K_{Ic} vs. temperature trend exactly, there appear to be simple solutions to these problems. The approach for improving the SSYCSM model was described in Section 3.8 of this report.

All of the models considered in this study assume that the WPS phenomenon is due to plasticity and residual stress effects in the crack tip region. While the details of the models are different, all of the models attempt to predict how these residual fields change the relationship between the remote applied load (or applied K) and the "effective K" being felt by the crack tip. Since none of the simple models, including the SSYCSM involve incremental plasticity (as would be required for an accurate representation of the crack tip field under cyclic loading) these simple models are best regarded as engineering tools rather than rigorous mathematical models. As such, further theoretical work is needed to establish whether differences between the model predictions and data are due to the approximate methods for modeling crack tip plasticity effects or due to other fundamental assumptions of the models. It would also be advantageous to know under what circumstances the simplistic approach to plasticity effects used by the models is conservative or nonconservative.

This study did not use irradiated material but is expected to be relevant to vessel material that has been exposed to fast neutron flux. The basis for this is that the principal effects of irradiation are to raise the yield stress of the material and reduce the toughness. It has been shown in the literature and has been verified in this study, that the critical stress criterion for cleavage fracture can reasonably predict the toughness reduction due to irradiation merely by knowing the increase in the yield stress. Therefore, it appears the toughness reduction is not an independent phenomena but is a consequence of the change in yield stress. Since reduced temperatures cause an increase in the yield stress in a manner

similar to irradiation, the present study assumes that irradiation effects are entirely analogous to the effects of reducing temperatures. Experiments to verify this experimental approach for WPS testing remain to be done.

4. CONCLUSIONS

Two goals of this project were to quantify the WPS phenomenon and to show its relevance to faulted conditions such as LOCA and PTS. The experimental results have shown, with due attention to statistical methods, that WPS can result in failure loads which are significantly greater than those that would be predicted using straight forward linear elastic fracture mechanics analysis. For the worst case LUCF load history, the average experimental K_f values were 1.6 to 2.5 times the virgin material K_{Ic} depending on the temperature at failure. For the LPUCF load history the average experimental K_f value was about three times K_{Ic}, and K_{wps} was effectively the lower bound of the K_f values.

The idealized LUCF and LPUCF load histories used in this study were not intended to be exact reproductions of real or postulated LOCA or PTS load histories. However, the WPS temperature and the WPS stress intensity level were selected to be representative of what might be encountered under PTS conditions and the idealized load histories are believed to be conservative approximations to actual or postulated LOCA or PTS load histories. The SSYCSM model predicts for example that by doing all unloading at the warm prestress temperature (Tmin = Twps) experimental failure loads will be smaller than for load histories which involve a simultaneous unloading and cooling.

The task to evaluate WPS predictive models resulted in the SSYCSM model being judged as most promising. In the process of reaching this conclusion, numerous other models and fracture criteria were considered. All of the other models and criteria were found to be either less accurate (J_e, dCTOD * FLOW, T_p^*, compact specimen strip yield model), less general in their applicability (J_e, compact specimen strip yield model), or did not have a sound physical basis (J_e).

5. SUGGESTIONS FOR FURTHER STUDY

Although the present study involved a substantial number of WPS tests, the variables covered were few because of the many duplicate specimens required to provide a firm basis for statistical analysis. Only three WPS load histories were actually considered. It is suggested that this matrix of WPS levels and test temperatures be expanded. Based on the results of the present work, it appears the number of duplicate specimens could be reduced without significantly reducing the accuracy of the statistical analysis.

This study used non-irradiated material but accounted for irradiation effects by doing tests at temperatures for which the yield strength and K_{Ic} behavior of the test material are believed to be representative of irradiated material. Because the accuracy of this approach has not been experimentally verified for WPS behavior, it is suggested that sufficient WPS testing be conducted with irradiated material to demonstrate the relevance to the tests done on non-irradiated material. Since it is conceivable that irradiation could interact with WPS behavior in other ways than through the yield strength and toughness, it would be most conclusive if warm prestress loading of the fracture specimens was either applied before or during irradiation.

The following suggestions for further model development work are based on the general conclusion that the critical stress criterion offers the most promise as a WPS fracture criterion:

i) While the simplistic superposition approach of Curry offers an attractively simple method for applying the critical stress criterion to WPS, it should be emphasised that solutions will generally differ from those which would be obtained using a more rigorous, incremental plasticity solution procedure. It is therefore recommended that the simplistic superposition approach be compared to the incremental, elastic-plastic approach so as to determine the effect on the accuracy of the predicted WPS failure loads.

ii) Since it is convenient for a WPS model to use standard K_{Ic} data as input rather than critical stress and distance, it is suggested that methods for determining the critical stress parameters from K_{Ic} data be further investigated.

iii) It appears that WPS behavior is primarily the results of elastic-plastic behavior at the crack tip. While the SSYCSM accounts for the elastic-plastic stress-strain behavior by assuming a Ramberg-Osgood type of power law, (which may in part explain the model's improved accuracy over strip yield based models), little is known about the sensitivity of the results to the hardening exponent of this law or to the quality of the fit between the assumed power law and the actual material behavior.

iv) There is some question as to the accuracy of the Tracy solution used in the SSYCSM. If these solutions are to be used in future work, it seems that their accuracy should be verified.

REFERENCES

1. R. B. Stonesifer and E. F. Rybicki, "Development of Models for Warm Prestressing," USNRC Report NUREG/CR-4491, MEA-2122, June 1986.

2. F. J. Loss, R. A. Gray, Jr. and J. R. Hawthorne, "Significance of Warm Prestress to Crack Initiation During Thermal Shock," Naval Research Lab. Report NRL-8165, Sept. 29, 1977.

3. F. J. Loss, R. A. Gray, Jr. and J. R. Hawthorne, "Investigation of Warm Prestress for the Case of Small Delta T During a Reactor Loss-of-Coolant Accident," Naval Research Lab. Report NRL-8198, March 9, 1978.

4. G. G. Chell, J. R. Haigh and V. Vitek, "A Theory of Warm Prestressing: Experimental Validation and the Implications for Elastic Plastic Failure Criteria," Int. J. of Fracture, Vol. 17, 1981, pp. 61-81.

5. B. A. Bilby, A. H. Cottrell, and K. H. Swinden, "The Spread of Plastic Yield from a Notch," Proc. Roy. Soc. A 272, 1963, p. 304.

6. D. S. Dugdale, "Yielding of Steel Sheets Containing Slits," J. Mech. Phys. Vol., 8, 1960.

7. D. A. Curry, "A Micromechanistic Approach to the Warm Prestressing of Ferritic Steels," CERL Lab Note RD/L/N103/79, Sept. 1979, Central Electricity Research Laboratories, Leatherhead, Surry, U.K.

8. D. M. Tracy, "Finite Element Solutions for Crack-Tip Behavior in Small-Scale Yielding," Trans. ASME, J. Eng. Mat. Tech., Vol. 98, 1976, pp. 146-151.

9. J. R. Rice, Fatigue Crack Propagation, ASTM STP 415, American Society for Testing and Materials, Phila., PA, 1967, p. 247.

10. B. A. Bilby, 3rd International Conference on Fracture, Munich, Part XI, PL1-111, Verein Deutscher Eisenhuttenlente, Dusseldorf (1973) 1-20. 1973.

11. H. Miyamoto and K. Kageyama, Proceedings 1st International Conference on Numerical Methods in Fracture Mechanics, Eds. A. R. Luxmore and D. R. J. Owen, Swansea University (1978) 479-486.

12. H. Miyamoto, K. Kageyama, M. Kikuchi, and K. Machida, "The Jext-Integral Based on the Concept of Effective Energy Release Rate," Elastic-Plastic Fracture: Second Symposium, Volume I - Inelastic Crack Analysis, ASTM STP 803, American Society for Testing and Materials, Phila., PA, 1983.

13. J. D. Eshelby, "The Continuum Theory of Lattice Defects," Solid State Physics, Vol. III, 1966.

14. G. P. Cherepanov, "Crack Propagation in Continuous Media," Journal of Applied Mathematics and Mechanics, English Translation, Vol. 31, 1967.

15. J. R. Rice, "A Path-Independent Integral and the Approximate Analysis of Strain Concentration by Notches and Cracks," J. Appl. Mech., Vol. 35, 1968.

16. S. N. Atluri, T. Nishioka, and M. Nakagaki "Incremental Path-Independent Integral in Inelastic and Dynamic Fracture Mechanics," Engrg. Fracture Mech., Vol. 20(2), 1984, pp. 209-244.

17. F. W. Brust, "The Use of New Path Independent Integrals in Elastic-Plastic and Creep Fracture," Ph.D. Thesis, Georgia Institute of Technology, 1984.

18. E. Orowan, "Fracture and Strength of Solids," Rep. Prog. Phys., 12, 1948, p. 185.

19. A. P. Green and B. B. Hundy, "Initial Plastic Yielding in Notch Bend Tests," J. Mech. Phys. Solids, 4, 1956, p. 128.

20. R. O. Ritchie, J. F. Knott and J. R. Rice, "On the Relationship Between Critical Tensile Stress and Fracture Toughness in Mild Steel," J. Mech. Phys. Solids, Vol. 21, 1973, p. 395.

21. D. M. Parks, "Interpretation of Irradiation Effects on the Fracture Toughness of a Pressure Vessel Steel in Terms of Crack Tip Stress Analysis," Trans. ASME, J. Eng. Mat. Tech., Vol. 98, 1976, pp. 30-36.

22. J. W. Hutchinson, "Singular Behavior at the End of a Tensile Crack in a Hardening Material," J. Mech. Phys. Solids, Vol 16, 1968, p. 13.

23. J. R. Rice and G. F. Rosengren, "Plane Strain Deformation Near a Crack Tip in a Power-Law Hardening Material," J. Mech. Phys. Solids, Vol. 16, 1968, p. 1.

24. D. M. Parks, "Some Problems in Elastic-Plastic Finite - Element Analysis of Cracks," Ph.D. Dissertation, Brown University, 1975.

25. J. R. Rice and E. P. Sorensen, "Continuing Crack-Tip Deformation and Fracture for Plane-Strain Crack Growth in Elastic-Plastic Solids'" J. Mech. Phys. Solids, Vol. 26, 1978, p. 163.

26. J. C. Newman Jr. and S. Mall, "Dugdale Plastic Zone Size and CTOD Equations for the Compact Specimen," Int. J. of Fracture, Vol. 24, 1984, p. R59.

27. J. C. Newman Jr., "Prediction of Stable Crack Growth and Instability Using the VR-Curve Method," Elastic-Plastic Fracture Mechanics Technology, ASTM STP 896, American Society for Testing and Materials, Phila., 1985, p. 139.

28. R. Hill, The Mathematical Theory of Plasticity, Oxford University Press, 1950.

29. R. M. McMeeking, "Finite Deformation Analysis of Crack Tip Opening in Elastic-Plastic Material and Implications for Fracture Initiation," J. Mech. Phys. Solids, Vol. 25, 1977, p. 357.

30. C. F. Shih, "Relationships Between the J-Integral and the Crack Opening Displacement for Stationary and Extending Cracks," J. Mech. Phys. Solids, Vol. 29, 1982, p. 305.

31. R. B. Stonesifer, "Fast-Brittle-Fracture and Creep Crack Growth: Moving Singularity Finite Element Analysis," Ph.D. Dissertation, Georgia Institute of Technology, 1981.

32. M. F. Kanninen and C. H. Popelar, Advanced Fracture Mechanics, Oxford University Press, 1985.

33. V. Kumar, M. D. German, and C. F. Shih, "An Engineering Approach for Elastic-Plastic Fracture Analysis," Topical Report No. EPRI NP-1931, Research Project 1237-1, Electric Power Research Institute, July, 1981.

APPENDIX A

TEST PROCEDURE AND ANALYSIS FOR K_f

1. TEST PROCEDURE

The specimens used to simulate warm prestress cycles were the 4T compact specimen geometry shown in Fig. A.1. All were 50.8-mm (2-in.) thick. No side grooving was used except for the two specimens selected from the LPUCF series, as noted in the text. A clip gage was attached on the load-line so that the area under the load-displacement records would correspond to the work done on the specimens. The objective was to warm prestress load to K_{wps} = 192 MPa$\sqrt{m}$ using J-integral and the conversion Eq. 1. A computer program was used that calculates J at stopping points where partial unloading is introduced for the measurement of the current crack size. The operator used these updated J calculations to decide when warm prestress loading should be discontinued. There of course had to be some small variability introduced into K_{wps} from this incremental loading process. A circulating air type furnance was used to heat each specimen to 177°C for warm prestressing. Temperature was controlled within ± 2°C. An HP 9845 desk-top computer was used to acquire data, record the data on floppy discs and compute J values. A special high-temperature type clip gage was used to measure load line displacement. Stroke control loading was used to prevent ductile instability.

For LUCF cycles, all specimens were K_{wps} loaded and completely unloaded at 177°C. They were then cooled to room temperature and were usually stored for several weeks prior to the loading to fracture part of the cycle. For K_f testing, a box with circulating LN vapor was used. Test temperatures were either -23°C or -95.5°C. Again, the loading mode was stroke control.

For LPUCF cycles, a special atmospheric control box was made that was capable of the temperature extremes used, viz 177°C to -95.5°C. K_{wps} loading was performed under stroke control, then switched to load control for the 1/3 partial unload and cooling of the system. After an appropriate soak time was allowed at the K_f test temperature, control was reverted back to stroke and the test completed to failure.

2. ANALYSIS FOR K_f

The reloading to failure at K_f temperatures always gave essentially linear load vs. displacement behavior. However, the K_{wps} loading gave the expected nonlinear test records such that elastic-plastic fracture mechanics was necessary to reflect the presence of plasticity and residual stresses from the WPS loading. When calculating K_f, test record linearity should not be interpreted as not indicating an absence of plasticity and the use of linear elastic fracture mechanics would be misleading. The method adopted here for calculating K_f results gives significantly higher K_f values.

As described previously, K_{wps} was obtained from J_{wps} using:

$$K_{wps} = \sqrt{J_{wps} E} \tag{1a}$$

where J_{wps} was determined from the experimental load deflection record using ASTM E 1152-87 procedures.

During unloading, it is assumed that the specimen deformation is predominately linear elastic (as suggested by the test records) and that the effective applied K during unloading is given by:

$$K = K_{wps} - \left[1 - \frac{P}{P_{wps}}\right] K_{wps}^{elastic} \tag{2a}$$

where P_{wps} is the load at WPS, P is the load during unloading ($P <= P_{wps}$),

$$K_{wps}^{elastic} = \frac{P_{wps}}{BW^{1/2}} f\left(a_p/W\right) \tag{3a}$$

is the linear elastic relation between the warm prestress load and K_I for an ideally elastic compact specimen, and a_p is the physical crack size. Therefore, the effective applied K at the unloaded or partially unloaded condition is given by

$$K_{min} = K_{wps} - \left[1 - \frac{P_{min}}{P_{wps}}\right] K_{wps}^{elastic} \tag{4a}$$

If P_{min} is zero (i.e., LUCF) then

$$K_{min} = K_{wps} - K_{wps}^{elastic} \tag{5a}$$

and it is seen that the effective applied K at the unloaded state is not zero. Only if the specimen is large enough that the load record is linear during the WPS loading will K_{min} be zero for a zero applied load.

Since the load records are observed to be linear during reloading to failure, it is again assumed that specimen behavior is predominately linear elastic, and thus Eq. 2a can also be used to determine the effective applied K during reloading and at the point of failure. Therefore

$$K_f = K_{wps} - \left[1 - \frac{P_f}{P_{wps}}\right] K_{wps}^{elastic} \tag{6a}$$

where P_f can be larger than P_{wps} and thus K_f can exceed K_{wps}. The observation that load deflection behavior remains linear for loads which are larger than P_{wps} can perhaps be attributed to the higher yield strength (and thus reduced plasticity) at the lower temperatures associated with the loading to failure.

Figure 11 in the body of the report illustrates the behavior assumed by Eq. 2a. Basically, Eq. 2a results in a linear K vs. load curve which passes through the (K_{wps}, P_{wps}) point and is parallel to the curve defined by the linear elastic behavior of Eq. 3a.

The nonlinear K versus P relation of Fig. 11 is based on a plastic zone correction to the linear elastic formula wherein a_p is replaced by an effective crack size a_e where

$$a_e = a_p + r_y \tag{7a}$$

and

$$r_y = \frac{1}{\beta\pi}\left(\frac{K}{\sigma_y}\right)^2 \tag{8a}$$

where β is typically taken to be 2 for plane stress and 6 for plane strain. Figure A.2 compares this simple approximation to the WPS data of this study and to results using the elastic-plastic estimation formulas from Ref. 33. It is seen that this formula and the experimental data are in good agreement and are also in good agreement with the plane strain trend predicted by the handbook. A best fit of the data with Equation (8a) was found to result in $5.7 \leq \beta \leq 6.4$ for all specimens without side grooves. The two side grooved specimens had a best fit β of 7.2. Since only two side grooved specimens were used, this slightly higher β may not be significant.

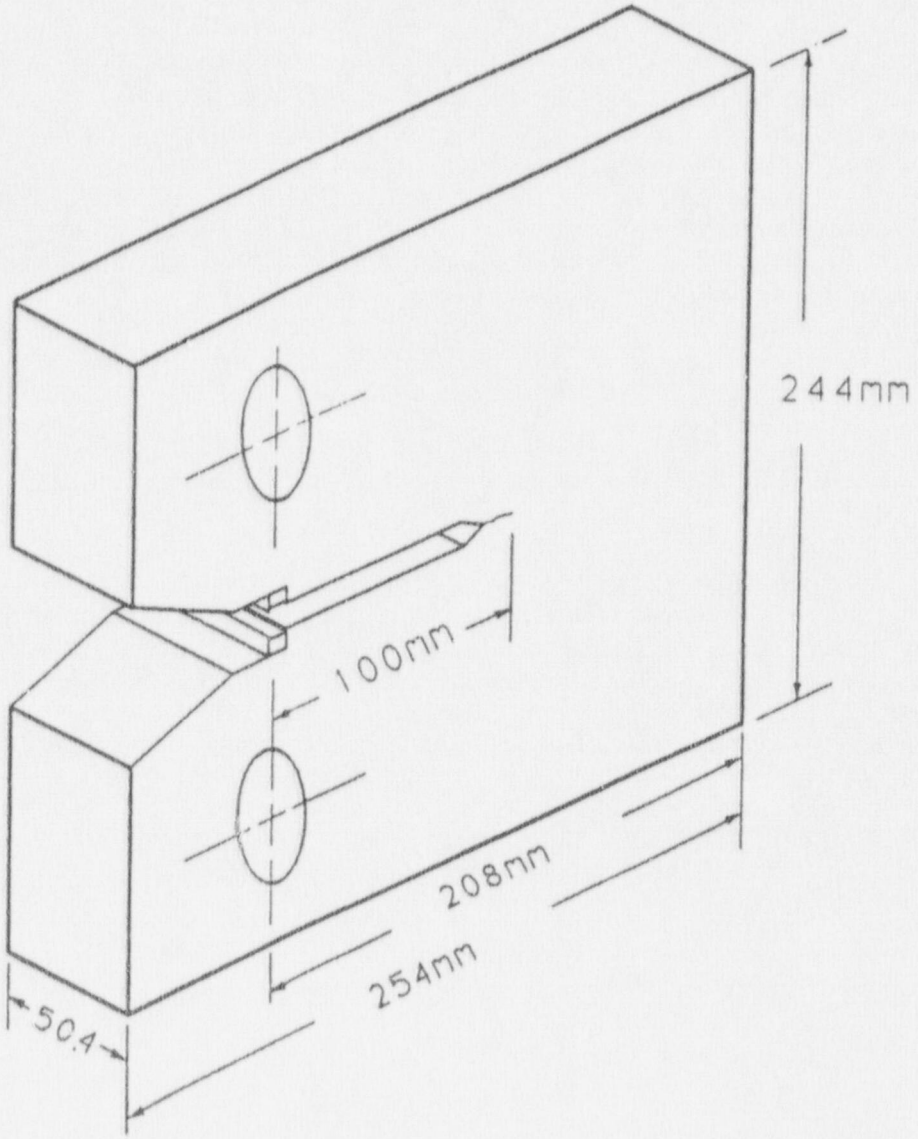

Fig. A.1 Sketch of 4T compact specimen used in the WPS study.

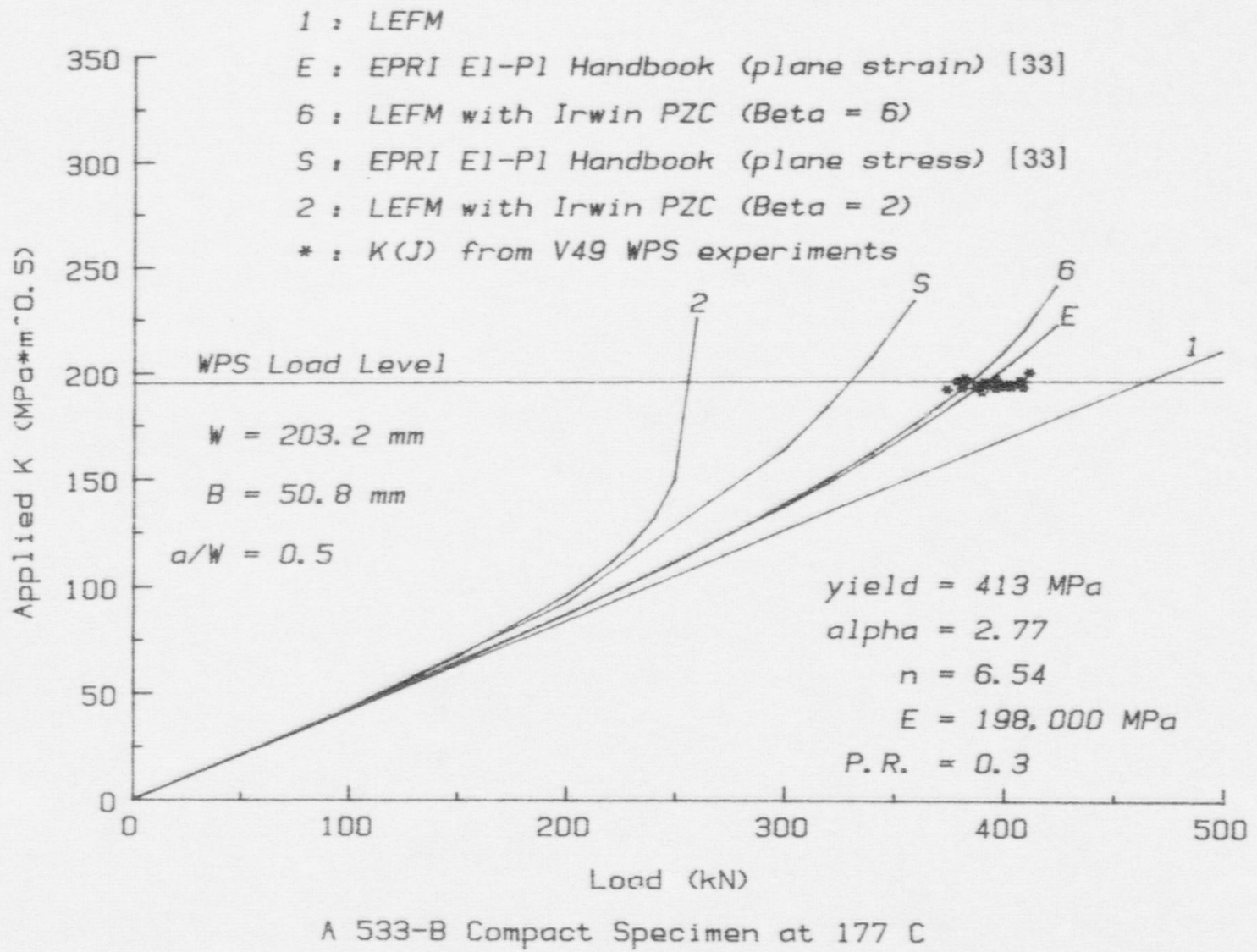

Fig. A.2 Load vs. applied K for five methods of elastic-plastic analysis. A comparison to experimental results.

APPENDIX B

FURTHER DISCUSSION ON WPS MODELS AND RELATED FRACTURE CRITERIA

1. SMALL SCALE YIELD STRIP YIELD MODEL RESULTS

The J_e criterion and the dCTOD * FLOW criterion have been used with both the small scale yield, strip yield model and the compact specimen strip yield model. Each model is used to predict WPS behavior for the experimental WPS load histories considered in this study plus a partial unloading (LPUCF) history in which failure occurs at -23.3°C for which experimental data was not developed. Each WPS load history was simulated using three assumed material toughness trends as input. One trend was intended to be a mean toughness trend while the other two are upper and lower bounds based on the K_{Ic} testing of this study at -23.3°C and -95.6°C.

The models use the average specimen crack size and K_{wps} for each set of duplicate specimens. Typically, variation in crack size among duplicate specimens was less than 0.5%, and variation in K_{wps} less than 3%. The LUCF simulations assume a K_{min} of 33 MPa$\sqrt{m}$, and the LPUCF simulations assume a K_{min} of 136 MPa$\sqrt{m}$. The K_{min} values for the LUCF history are slightly larger than the average experimental values (30 MPa$\sqrt{m}$ at -95.6°C and 32 MPa$\sqrt{m}$ at -23.3°C). This discrepancy is not believed to have a significant effect on the results and conclusions of this study.

Figure B.1 compares the WPS K_f predictions with the experimental LUCF data using J_e and dCTOD * FLOW as a fracture criteria. It is seen that the predicted failure values tend to be conservative at -95.6°C. Generally, the predictions based on J_e tend to be in better agreement with the data than those based on dCTOD * FLOW.

While adjusting the constraint factor might be expected to improve the strip yield model predictions based on the behavior of the critical stress model discussed in Section 3.7, this is not the case. The small scale yield, strip yield model predictions using J_e or dCTOD * FLOW are independent of the flow stress in a manner similar to small scale yield (LEFM) K formulas being independent of flow (or yield) stress.

Figures B.2 compares the WPS K_f predictions with the experimental LPUCF data using J_e and dCTOD * FLOW as fracture criteria. While the dCTOD * FLOW predictions were found to be less accurate than those due to J_e in Fig. B.1 (LUCF), the opposite appears to be true for Fig. B.2 (LPUCF). The present lack of experimental data at -23.3°C, however, makes this a tentative conclusion.

2. COMPACT SPECIMEN STRIP YIELD MODELS

Due to the departure from small scale yielding at K_{wps} in the present experiments and the subsequently required assumptions on applied K vs. load behavior, it was anticipated that the use of the non-small scale

yield strip yield model of Newman and Mall (for the compact specimen) would improve the J_e and dCTOD * FLOW based predictions. However, as mentioned previously, the predictions were found to be clearly less accurate than those using the small scale yield model.

Figure B.3 compares experimental (LUCF) failure loads with those using J_e and the compact specimen strip yield model. As a result of this not being a small scale yielding model, it is seen that the results are dependent on the selected constraint factor. It is also important to note that the predictions are in terms of actual loads rather than applied K. The compact specimen strip yield model of Newman and Mall uses plane stress solutions, therefore, constraint factors are greater than unity so as to reflect the larger constraint associated with plane strain. The constraint factor of 1.14 is considered to be the most appropriate value since it results in the K(J) from the model matching the K(J) from the experiment. The value of 1.73 (i.e., $\sqrt{3}$) is the customary value for plane strain.

It is clear that the higher constraint results in more accurate failure load predictions. However, as noted above, selecting the higher constraint results in unrealistic K vs. load behavior being predicted during the WPS loading. Considering Fig. B.3.b, and comparing with the similar plot for the small scale yield, strip yield model, (Fig. B.1.a) it can be seen that the agreement with the data is better when using the small scale yield model.

Figure B.4 compares experimental (LPUCF) failure loads with those using J_e and the compact specimen strip yield model. For this load history, the predicted failure loads are seen to be largely independent of constraint. Also, the results from using the compact specimen strip yield model are very similar to those using the small scale yield model (Fig. B.2.a)

Figure B.5 compares experimental (LUCF) failure loads with those using dCTOD * FLOW and the compact specimen strip yield model. It can be seen that the predictions using the dCTOD * FLOW criterion are much less sensitive to the constraint factor than those using J_e. This difference is believed to be related to the fact that dCTOD * FLOW is defined exclusively in terms of crack tip quantities while J_e is dependent on deformations at a significant distance from the crack tip. Comparing predictions using the compact specimen strip yield model with those using the small scale yield, strip yield model, (Fig. B.1.b) it is seen that more accurate predictions again result from using the small scale yield model.

Figure B.6 compares experimental (LPUCF) failure loads with those using dCTOD * FLOW and the compact specimen strip yield model. The predicted failure loads are again seen to be largely independent of constraint. Also, the results from using the compact specimen strip yield model are very similar to those using the small scale yield model. As a result of limitations on plastic zone sizes in the Newman and Mall strip yield model, some failure loads could not be predicted at the -23.3°C failure temperature.

When either the J_e or the dCTOD * FLOW criterion was used with the compact specimen strip yield model, the predictions were found to be less accurate than when using the small scale yield, strip yield model. If the compact specimen model is indeed more representative of the deformation behavior of the experimental specimens than the small scale yield model, then this behavior suggests that the less accurate failure predictions are the result of the fracture criteria.

Although it is believed that the less accurate predictions using the compact specimen model are the result of J_e and dCTOD * FLOW being inadequate WPS fracture criteria, the possibility of the fault being with the compact specimen model cannot be totally ruled out. One point of uncertainty is the effect of assuming plane stress rather than plane strain (as is customary for strip yield models) during the development of the model by Newman and Mall. It is not clear, particularly as a result of the inclusion of back face yielding correction factors, that constraint factors can effectively be used to alter the model behavior so as to be applicable to conditions other than plane stress.

3. FURTHER DISCUSSION ON THE SMALL SCALE YIELD CRITICAL STRESS MODEL (SSYCSM)

Small scale yield, finite element solutions (e.g., Refs. 1 and 8), ideally result in solutions which approach the elastic asymptotic solution at large distances from the crack tip compared to the plastic zone size. For distances which are small compared to the plastic zone, the crack tip field approaches a fully plastic asymptotic field (i.e., elastic strains are negligible compared to plastic strains). If the stress-strain relation is of the power-law hardening variety, then the fully plastic asymptotic field is the so-called HRR field (Refs. 22 and 23). The numerical (e.g., finite element) solution is needed to "fill-in" between the two asymptotic solutions.

Tracey summarizes the crack plane normal stresses from his small scale yield solutions as a family of curves which depend only on the hardening exponent. The ligament stress is normalized by the yield stress and is plotted as a function of distance from the crack tip where the distance (x) is normalized by $(K_I / \text{yield})^2$.

It is rather clear that such a small scale yield solution can be applied to a finite geometry such as a compact specimen, when its plastic zone is small compared to the other dimensions. However, it is not so clear what applicability the solution has, and thus what applicability the SSYCSM has, when the finite geometry is loaded beyond the small scale yield regime.

Figure B.7 shows the linear elastic and fully plastic ligament stress distributions for a standard compact specimen obtained in this study using the finite element formulation and special crack tip elements of Reference 31.

Figure B.7.b shows the stresses in the entire ligament while Fig. B.7.a concentrates on the crack tip region. The plane strain, fully plastic solution assumes a Ramberg-Osgood power-law stress-strain relation with a hardening exponent of n = 10. The elastic and fully plastic asymptotic solutions are obtained independently (Refs. 32 and 22, respectively) and serve as a verification of the accuracy of the numerical solutions.

Figure B.8 compares Tracey's small scale yield solution to the limiting elastic and fully plastic solutions for the compact specimen geometry. In converting from Tracey's nondimensional stress and distance to those of this figure, it was necessary to introduce the reference load Po. Po is an estimate of the limit load for the compact specimen geometry for plane strain conditions (Reference 33) and is proportional to the yield stress. (Note that the power-law hardening assumption precludes a real limit load, and therefore, Po is best considered as a reference load.) It can be seen that the Tracey solution provides a basis for interpolation between the elastic and fully plastic solutions with the interpolation parameter being P/Po. It can also be seen that in the region x/(W-a) smaller than 10^{-2} (i.e., 1%) the Tracey small scale yield solution appears to reasonably represent the crack tip stresses right up to the fully plastic condition despite the fact that small scale yield conditions would generally require P/Po to be less than about 0.5. It should be noted, however, that due to the log-log nature of the plot, significant percentage changes in the stress levels of the Tracey solution would not necessarily destroy the reasonableness of the interpolation.

Since the critical distance for the critical stress criterion has in general been found to be less than 0.1 mm for the material of this study, the condition that x/(W-a) be less than 1% suggests that W can be as small as 20 mm or roughly a 1/2T standard compact specimen.

For the purposes of the SSYCSM, however, it happens that this estimate of the smallest applicable specimen size represents a necessary condition rather than a sufficient condition. Other considerations require that a larger specimen be used. The reasons are essentially the same as outlined in Section 3.4. That is, in order to apply the small scale yield model, it is necessary to relate the applied K of the model to the actual applied load. While the initial load (i.e., the WPS load) exceeding small scale yield can be tolerated as a result of the availability of elastic-plastic estimates for J (or K), the plasticity associated with the subsequent unloading and reloading to failure must be within the limits of small scale yielding in order that an applied K can reasonably be estimated. This restriction results from current elastic-plastic fracture methods (J based) dependence on monotonic loading. The requirement for small scale yielding during unloading and reloading will generally require a much larger specimen (or smaller load) than the above $x/(W-a) < 10^{-2}$ requirement. The present work using half thickness 4T specimens seems to suggest that for load levels considered in this study, the use of smaller specimens may not be possible if the SSYCSM is to be applied.

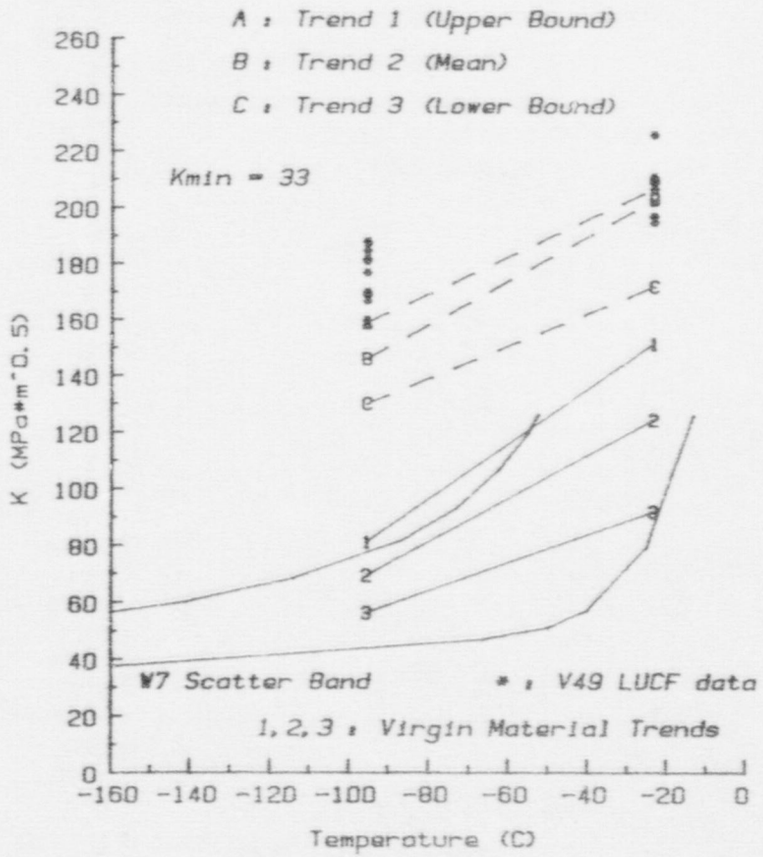

a. Je / Small Scale Yield Model

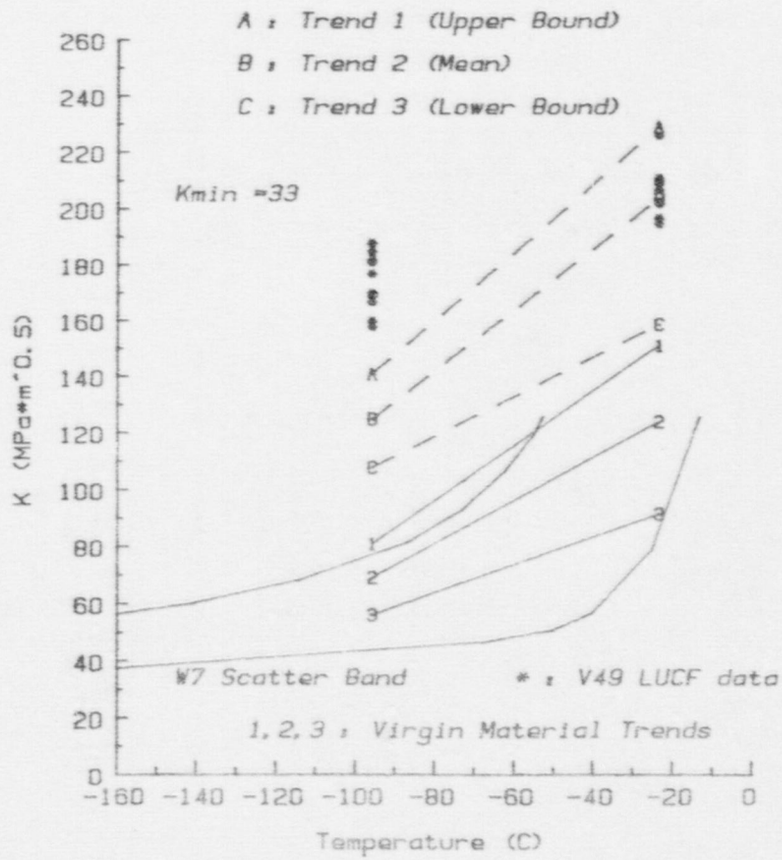

b. dCTOD * FLOW / Small Scale Yield Model

Fig. B.1 Comparison of experimental and predicted K_f for the LUCF WPS load history using the small scale yield, strip yield model with the J_e and dCTOD * FLOW fracture criteria.

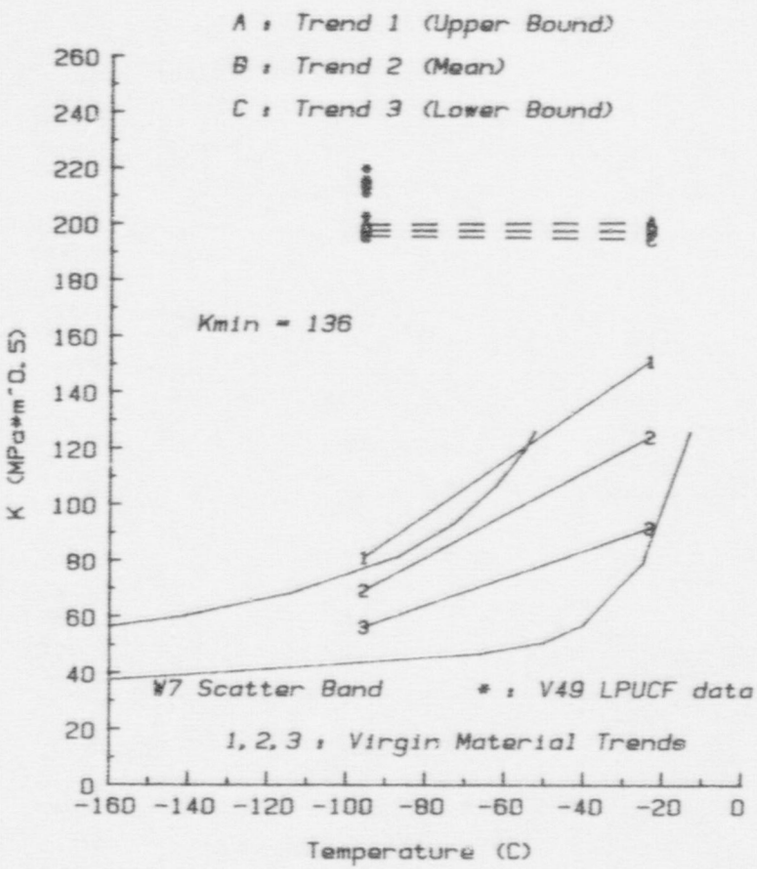

a. Je / Small Scale Yield Model

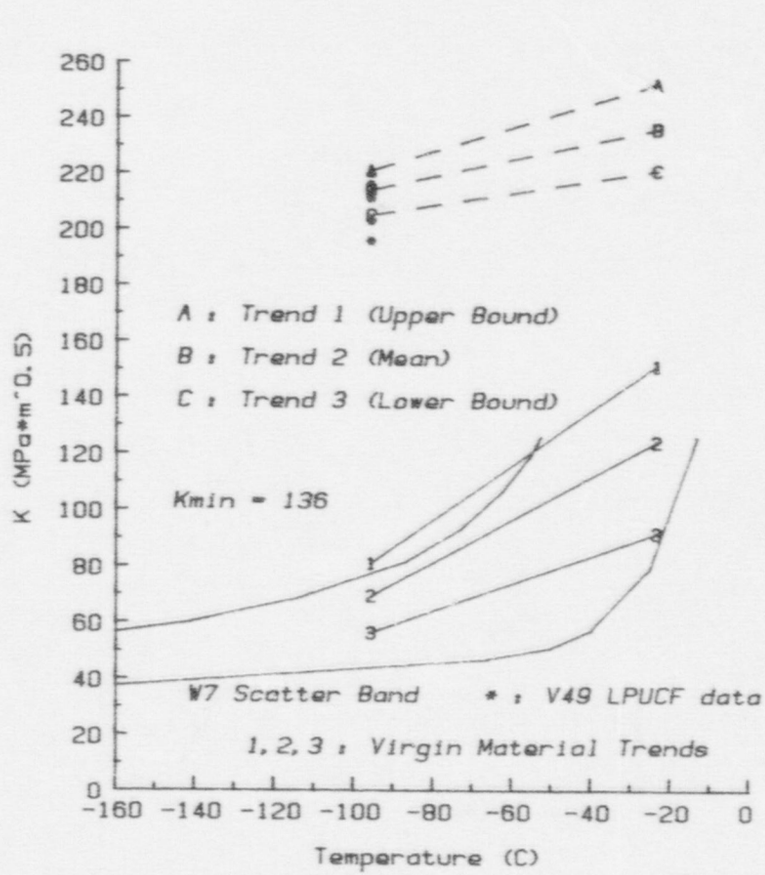

b. dCTOD * FLOW / Small Scale Yield Model

Fig. B.2 Comparison of experimental and predicted K_f for the LPUCF WPS load history using the small scale yield, strip yield model with the J_e and dCTOD * FLOW fracture criteria.

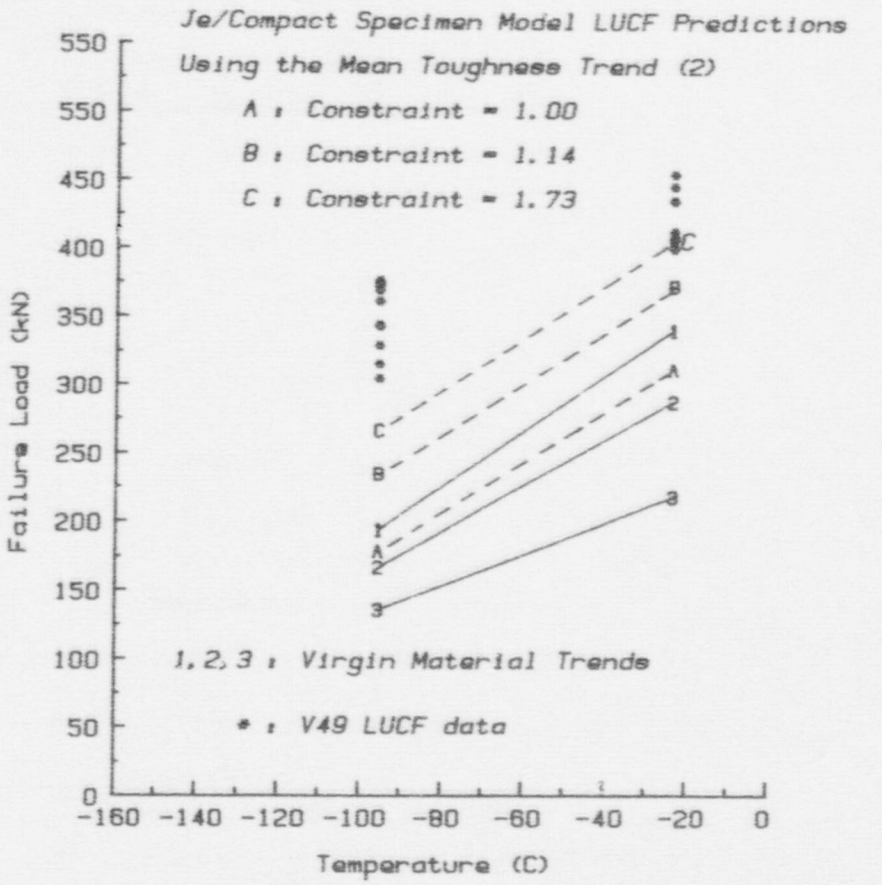

a. Effect of Constraint

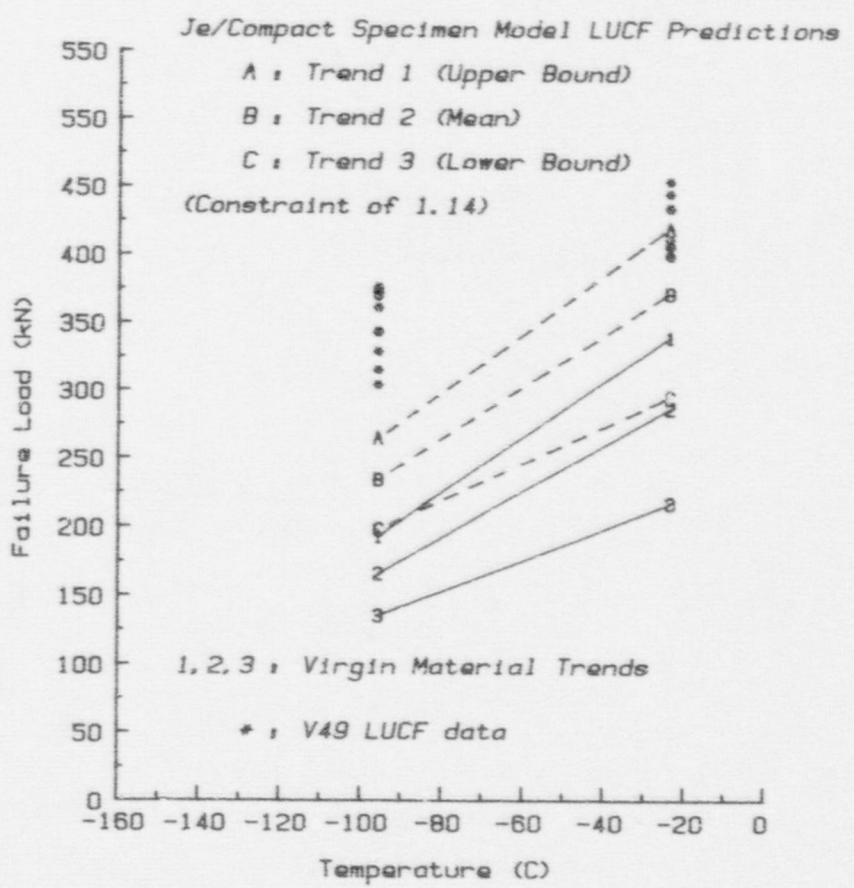

b. Effect of Virgin Material Trend

Fig. B.3 Comparison of experimental and predicted failure loads for the LUCF WPS load history using j_e with the compact specimen strip yield model.

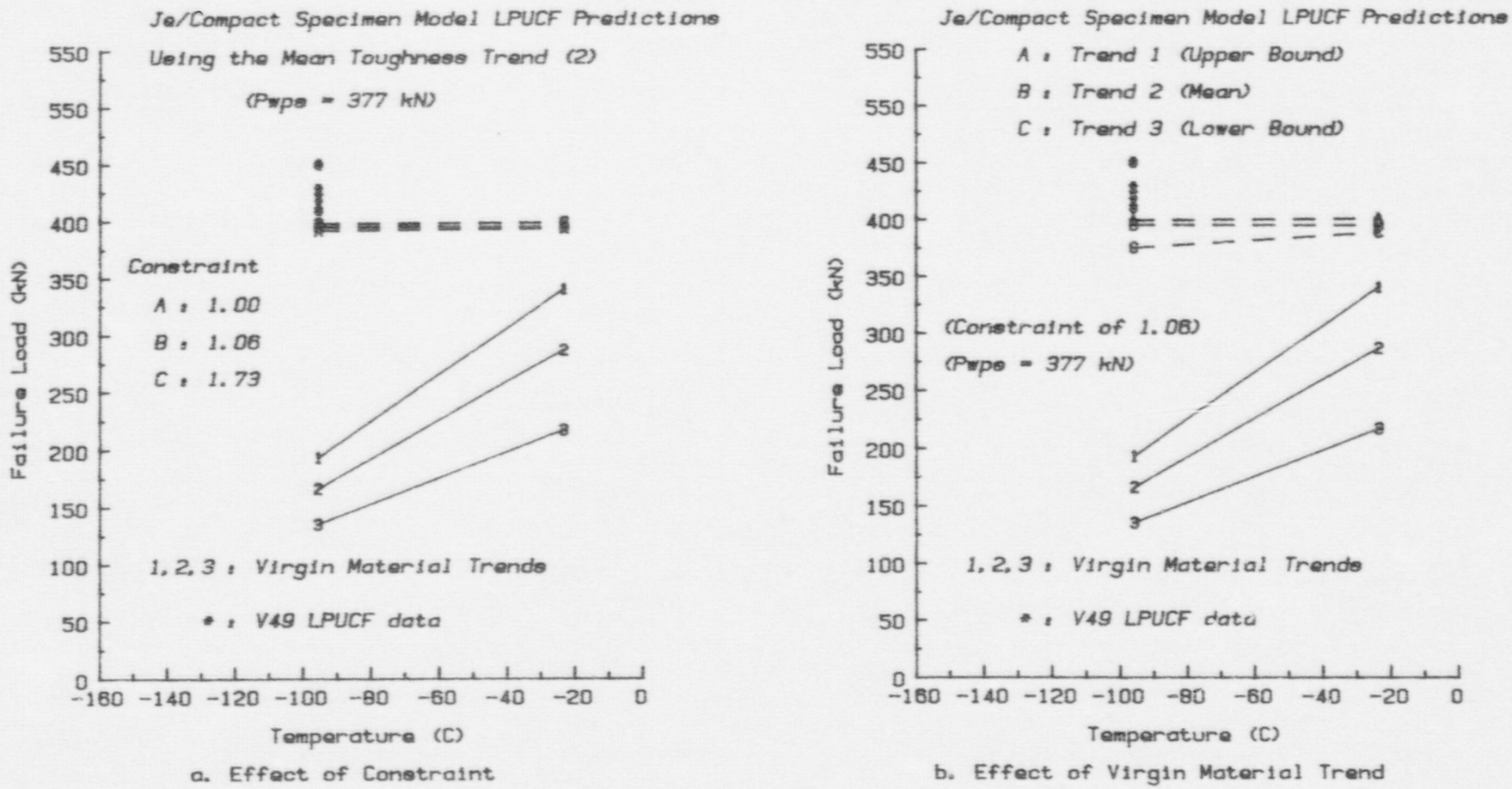

Fig. B.4 Comparison of experimental and predicted failure laods for the LPUCF WPS load history using J_e with the compact specimen strip yield model.

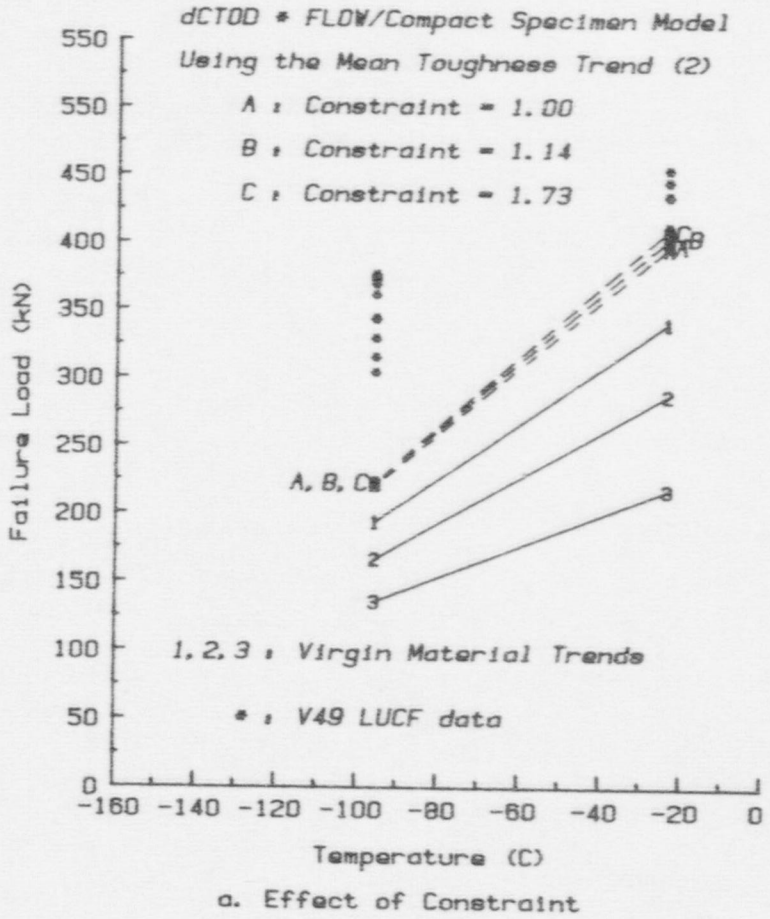

a. Effect of Constraint

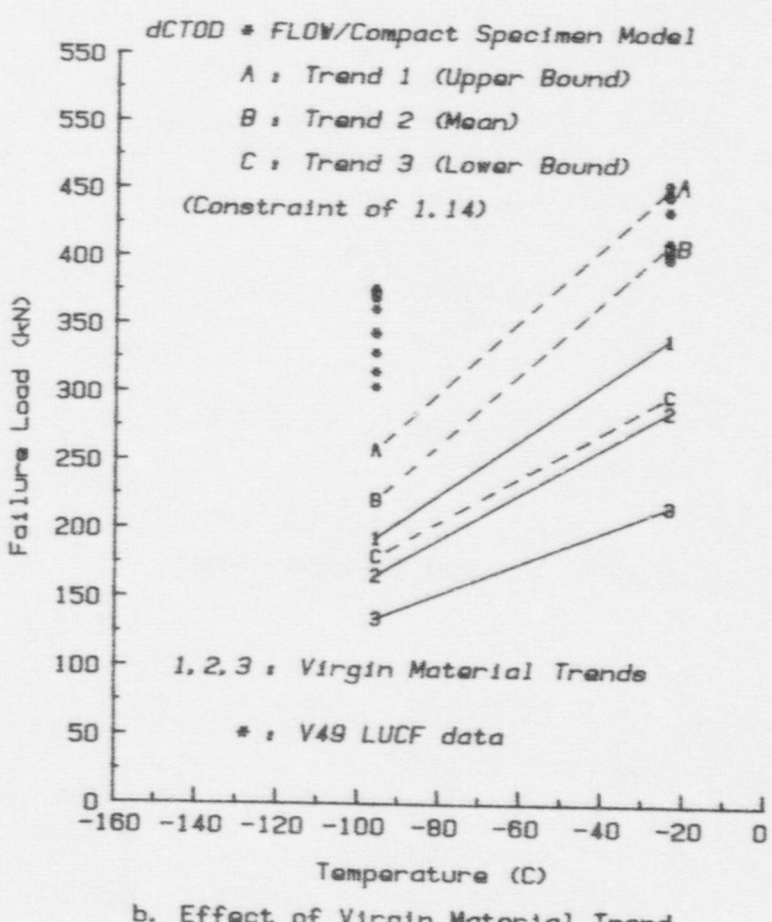

b. Effect of Virgin Material Trend

Fig. B.5 Comparison of experimental and predicted failure loads for the LUCF WPS load history using dCTOD * FLOW and the compact specimen strip yield model

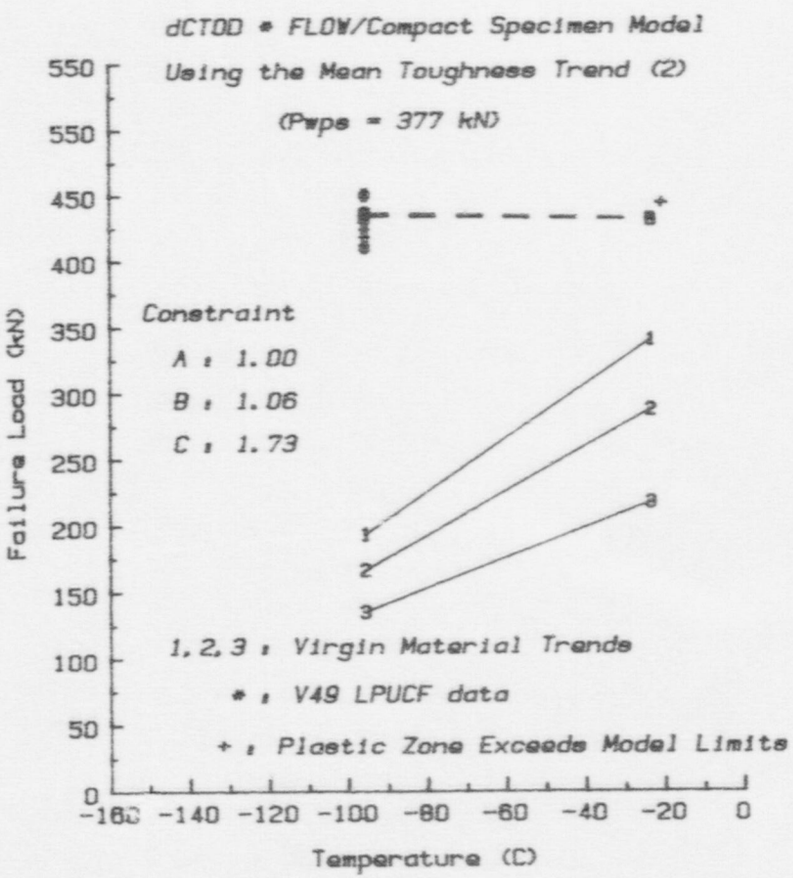

a. Effect of Constraint

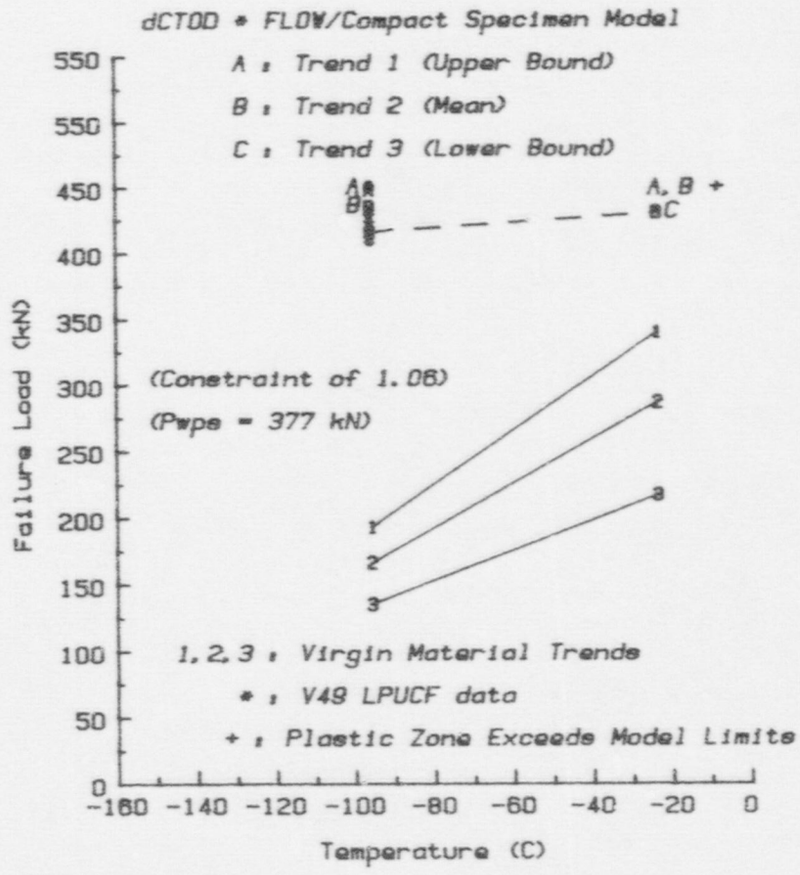

b. Effect of Virgin Material Trend

Fig. B.6 Comparison of experimental and predicted failure loads for the LPUCF WPS load history using dCTOD * FLOW and the compact specimen strip yield model.

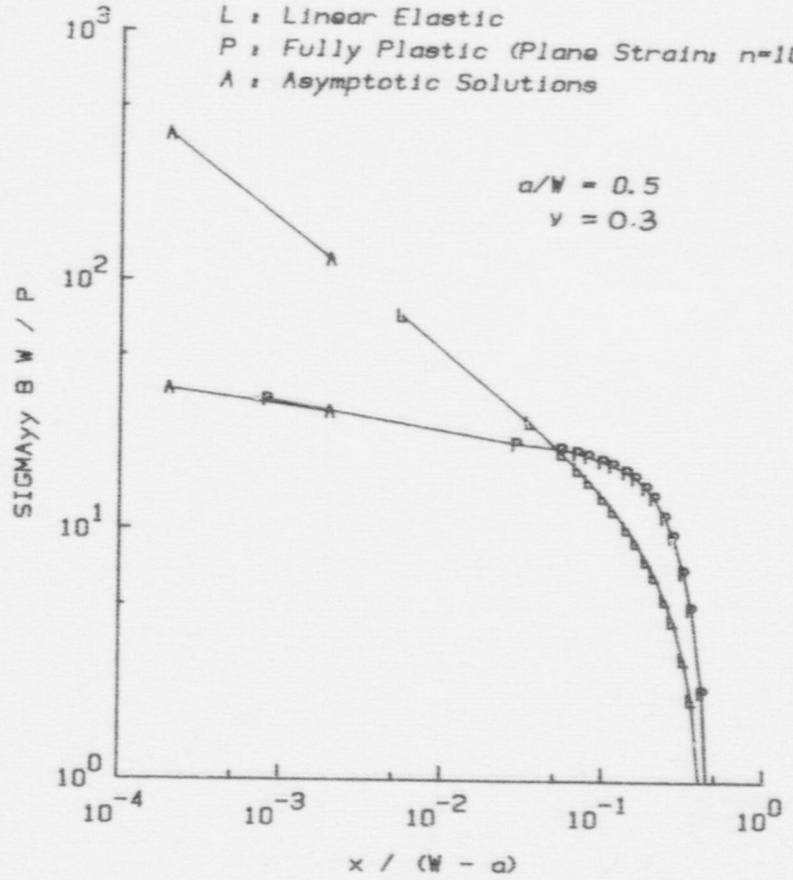

a. Comparison with Asymptotic Solutions

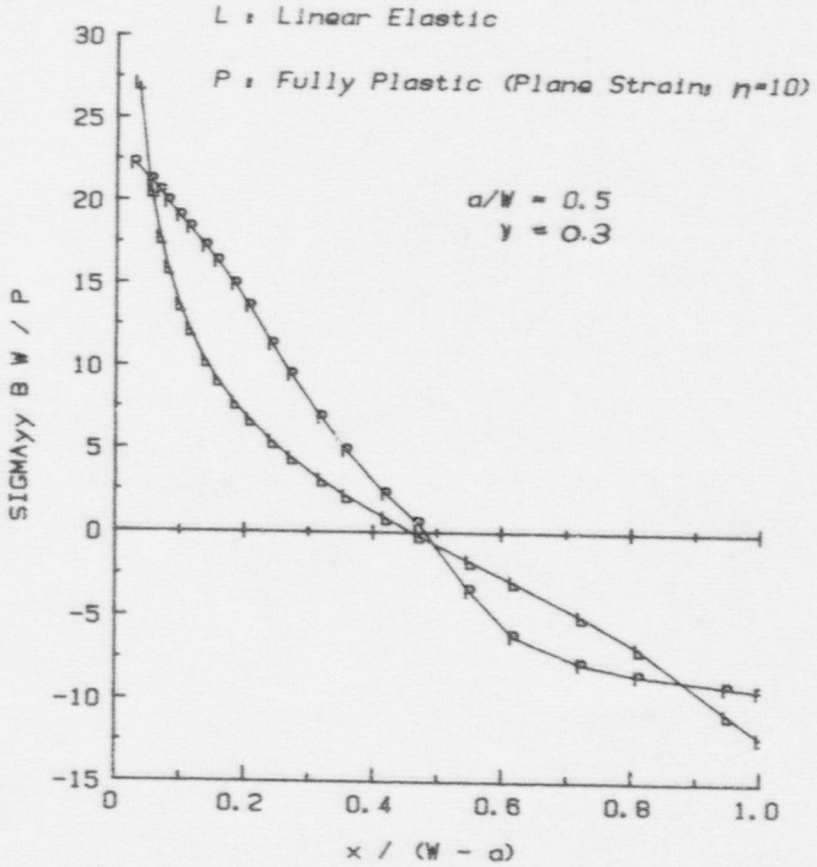

b. Computed Ligament Normal Stress

Fig. B.7 Ligament normal stress distribution for a standard compact specimen (X = 0 corresponds to the crack-tip.

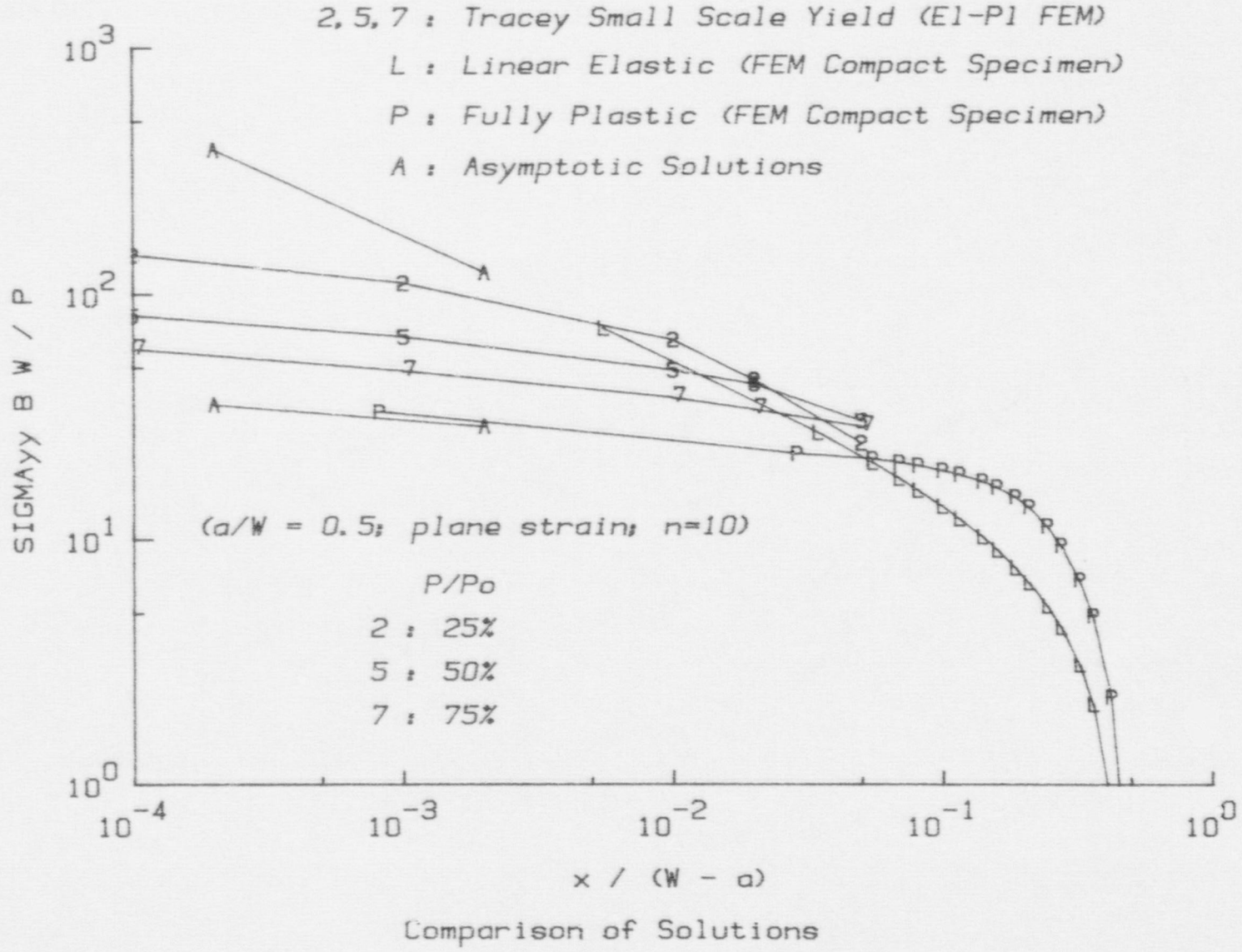

Fig. B.8 Tracey's crack plane stress distributions compared to the bounding elastic and fully plastic solutions for a standard compact specimen (X = 0 corresponds to the crack-tip).

NRC FORM 335 (11-81)

U.S. NUCLEAR REGULATORY COMMISSION

BIBLIOGRAPHIC DATA SHEET

1. REPORT NUMBER (Assigned by DDC)
NUREG/CR-5208
MEA-2305

4. TITLE AND SUBTITLE (Add Volume No., if appropriate)
Warm Prestress Modeling:
Comparison of Models and Experimental Results

2. (Leave blank)

3. RECIPIENT'S ACCESSION NO.

7. AUTHOR(S)
R. B. Stonesifer, E. F. Rybicki, D. E. McCabe

5. DATE REPORT COMPLETED
MONTH: January YEAR: 1989

9. PERFORMING ORGANIZATION NAME AND MAILING ADDRESS (Include Zip Code)
Materials Engineering Associates, Inc.
9700-B Martin Luther King, Jr. Highway
Lanham, Maryland 20706-1837

DATE REPORT ISSUED
MONTH: April YEAR: 1989

6. (Leave blank)

8. (Leave blank)

12. SPONSORING ORGANIZATION NAME AND MAILING ADDRESS (Include Zip Code)
Division of Engineering
Office of Nuclear Regulatory Research
U. S. Nuclear Regulatory Commission
Washington, DC 20555

10. PROJECT/TASK/WORK UNIT NO.

11. FIN NO.
B8900

13. TYPE OF REPORT
Technical Report

PERIOD COVERED (Inclusive dates)

15. SUPPLEMENTARY NOTES

14. (Leave blank)

16. ABSTRACT (200 words or less)

The objectives of this study were to develop warm prestress (WPS) data for which the enhanced toughness due to WPS could be separated from the statistical variability in K_{Ic} of the virgin material and to evaluate several candidate WPS models. Two types of loading sequences were load-unload-cool-fail (LUCF) and load-partial unload-cool-fail (LPUCF). The LUCF experiments showed 1.6 to 2.5 times K_{Ic} improvement over that of the low temperature K_{Ic} fracture toughness of virgin material. The LPUCF experiments showed about 3 times improvement over low temperature K_{Ic}. Mathematical WPS models of Chell, compact specimen strip yield model of Newman and Mall, and a small scale yield critical stress model SSYCSM of Curry were used to predict experimental WPS results. The SSYCSM model seemed to make the most sense on a physical basis and also provide the most accurate predictions. These results suggest that WPS effects deserve serious consideration in Loss of Coolant accident scenarios and in assessments applied to plant life extension considerations.

17. KEY WORDS AND DOCUMENT ANALYSIS

17a. DESCRIPTORS

Warm Prestress; LOCA; PTS; A 533-B
WPS Models; Transition Temperature

17b. IDENTIFIERS/OPEN-ENDED TERMS

18. AVAILABILITY STATEMENT
Unlimited

19. SECURITY CLASS (This report)
Unclassified

21. NO. OF PAGES

20. SECURITY CLASS (This page)
Unclassified

22. PRICE
$

NUREG/CR-5208

WARM PRESTRESS MODELING:
COMPARISON OF MODELS AND EXPERIMENTAL RESULTS

APRIL 1989